FEA of an Essentially Nonlinear Elastomeric Spring for a Nonlinear Energy Sink, Numerical Optimization and Performance Evaluation for Civil Structures

By

Muhammad Affan Zafar

(Registration No: 00000319092)

Department of Engineering

School of Interdisciplinary Engineering & Sciences

National University of Sciences & Technology (NUST)

Islamabad, Pakistan

(August 2023)

FEA of an Essentially Nonlinear Elastomeric Spring for a Nonlinear Energy Sink, Numerical Optimization and Performance Evaluation for Civil Structures

By

Muhammad Affan Zafar

(Registration No: 00000319092)

A thesis submitted to the National University of Sciences and Technology, Islamabad,

in partial fulfillment of the requirements for the degree of

Master of Science in Computational Science and Engineering

Thesis Supervisor: Dr. Absaar ul Jabbar

School of Interdisciplinary Engineering and Sciences

National University of Sciences & Technology (NUST)

Islamabad, Pakistan

(August 2023)

Annex A to NUST Letter No. 0972/102/Exams/Thesis-Cert dated 23 Dec 16.

THESIS ACCEPTANCE CERTIFICATE

Certified that final copy of MS/MPhil thesis written by Mr Muhammad Affan Zafar Registration No. 319092 of SINES has been vetted by undersigned, found complete in all aspects as per NUST Statutes/Regulations, is free of plagiarism, errors, and mistakes and is accepted as partial fulfillment for award of MS/MPhil degree. It is further certified that necessary amendments as pointed out by GEC members of the scholar have also been incorporated in the said thesis.

Signature with stamp: _____

Assistant Professor
SINES - NUST, Sector H-12
Islamabad

Name of Supervisor: DR. ABSAAR UL JABBAR

Date: 2-8-2023

Signature of HoD with stamp: _____

Dr. Mian Ilyas Ahmad
HoD Engineering
Professor
SINES - NUST, Sector H-12
Islamabad

Date: 03/08/2023

Countersign by

Signature (Dean/Principal): _____

Dr. Hammad M. Cheema
Principal & Dean
SINES - NUST, Sector H-12
Islamabad

Date: 08/08/2023

Declaration

I certify that this research work titled *"FEA of an Essentially Nonlinear Elastomeric Spring for a Nonlinear Energy Sink, Numerical Optimization and Performance Evaluation for Civil Structures"* is my own work. The work has not been presented elsewhere for assessment.

I confirm that:

1. This work was done wholly or mainly while in candidature for Master of Science degree at NUST.
2. Where any part of this thesis has been previously submitted for a degree or any other qualification at NUST or any other institution, this has been clearly stated.
3. Where I have consulted the published work of others, this is always clearly attributed.
4. Where I have quoted from the work of others, the source is always given. With the exception of such quotations, this thesis is entirely my own work.
5. I have acknowledged all main sources of help.
6. Where the thesis is based on worked done by myself jointly with others, I have made clear exactly what was done by others, and I have contributed myself.

_____

Muhammad Affan Zafar

00000319092

Copyright Notice

Acknowledgements

My foremost gratitude is reserved for my creator and sustainer Allah (S.W.T). Indeed, without His blessing, guidance and help, this accomplishment would not have been possible. It was He who made way for me in the blind alley and showed me light in the dark.

Secondly, I am eternally indebted to my mother who stuck with me through extremely trying times. Her support is invaluable in the completion of this study. I would also like to mention my sister who encouraged me throughout. Lastly, I must appreciate whosoever helped me throughout my thesis, especially my close friends Hasan Khawar and Talha Khan.

I would also like to express special thanks to my supervisor Dr. Absaar ul Jabbar for his commitment to see my thesis through to completion. I must also state my partiality for SINES NUST faculty and staff for contributing to my study in their own capacities.

Finally, I must also pay my regards to anyone who has contributed to my success in any way big or small as each piece of help was equally essential in this cause.

Dedicated to my beloved mother whose immense determination and unwavering support led me to attain this wonderful accomplishment.

Abstract

This study is conducted with the intention of contributing towards development of a transformable regime for Non Linear Energy Sinks used as Dynamic Vibration Absorbers for vibration mitigation in civil structures. It primarily deals with the finite element analysis of a hyper-elastic polyurethane foam under compression which behaves as an essentially nonlinear spring in a Nonlinear Energy Sink (NES). Previous studies have used Mooney-Rivlin model for compressive strains up to 40% for hyperelastic materials with geometric nonlinearities. Mooney-Rivlin model has the limitation that it can only be used to accurately simulate strains up to 50% and cannot accurately predict the 3 regions (linear, collapse and compaction) in an elastomeric compression. This study builds on the previous works by conducting an FEA analysis of a geometrically nonlinear hyperelastic material upto compressive strains of 80% using Ogden model.

A FEA simulation in ABAQUS is conducted for a truncated cone shaped elastomer under compression. Initially a widely used strain energy density-based model for elastomers in compression, Ogden, is evaluated under different strain energy potential orders. Secondly, height of the truncated cone is varied to document the effect of geometric parameter on stiffness under compressive loading. In the final phase, the force-displacement curve obtained from these studies is imported into ETABS as a characteristic of a nonlinear link. This link is attached to a 10-storey rigid frame structure whose story displacement plots are compared with and without the link to exhibit the effectiveness of this nonlinear spring element in mitigation of structural vibrations. The results demonstrate that the 3rd order Ogden model can be used for simulating large compressive deflections, up to 80% strain, in hyper-elastic polyurethane foam. It makes evident that the force-displacement graph of the material exhibits nonlinear behavior in 3 regions (linear, collapse and compaction) in force-deflection graph which can be utilized in applications as an essentially nonlinear spring in NES and finally that this type of device can mitigate the story displacement in civil structures.

Table of Contents

Chapter 1: Introduction

Nonlinear Energy Sinks

In recent years, the application of Dynamic Vibration Absorbers (DVAs) has expanded to include the use of nonlinear energy sink (NES) devices. These devices, which can have either one or two degrees of freedom, are attached to dynamic structures to mitigate vibrations using essentially nonlinear elements. Unlike conventional linear absorbers, NES devices incorporate essentially nonlinear spring components during the design phase. The term "essentially nonlinear spring" refers to springs that either lack or have negligible linear components, resulting in a load-displacement curve without any linear behavior.

NES devices have garnered attention due to their distinct characteristics compared to commonly employed linear absorbers. By utilizing essentially nonlinear spring components, these devices offer a new approach to vibration mitigation. Unlike other types of nonlinear springs, such as metallic dampers that exhibit elasto-plastic behavior, NES devices maintain their essentially nonlinear behavior throughout the entire load-displacement curve. This unique attribute allows them to effectively absorb and dissipate energy, thereby enhancing the overall damping capacity of the dynamic structure.

Researchers and engineers are actively studying NES devices to investigate their behavior and performance under different loading conditions. The aim is to optimize their design parameters and explore their potential applications. Understanding the dynamics and nonlinear behavior of NES devices is crucial for refining their designs and tailoring them to specific scenarios. This knowledge contributes to the

development of improved vibration control techniques, reducing potential damage and fatigue in structures across various industries.

The ongoing advancement of NES devices as nonlinear energy sinks within DVAs presents exciting prospects for vibration mitigation. These devices, with their essentially nonlinear spring components, offer a distinct alternative to traditional linear absorbers. By further exploring the capabilities and optimizing the design of NES devices, engineers can continue to enhance vibration control techniques, ultimately improving the durability and reliability of structures in diverse applications. (Luo, Wierschem, Fahnestock, Spencer, et al., 2014).

Types of NES's and their Advantages

NESs' are typically classified into the following categories based on their components and arrangement:

1. Type I NES has a small mass and is coupled to a structure with primarily linear behavior through a linear damping element and essentially nonlinear stiffness elements as shown in Figure 3.

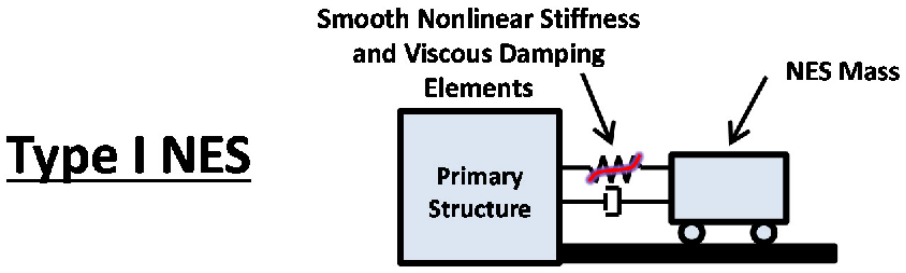

Figure 1 Type I NES (Nicholas E. Wierschem, 2014)

2. Type II NES is a more complex variation of the Type I NES where among the nonlinear stiffness element, the damping element also has nonlinear characteristics Figure 2.

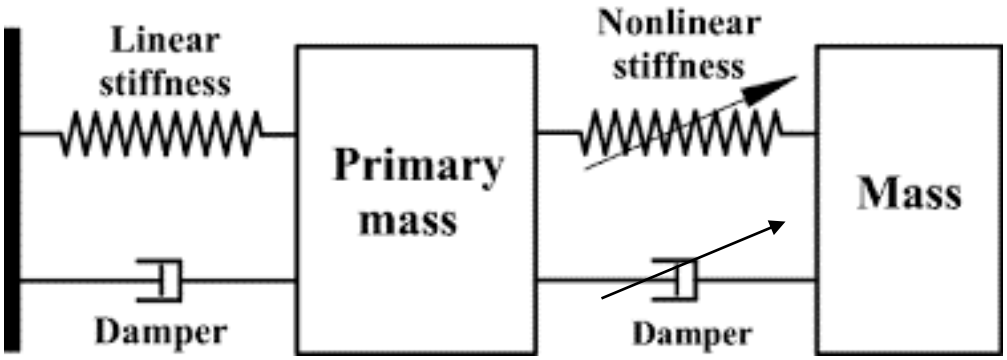

Figure 2 Type II NES (Ding & Chen, 2020)

3. Type III NES is the most complex type of device being studied. It is a two-degree freedom system as it has two masses. The upper NES mass is coupled to the bottom one through essentially nonlinear stiffness element, whereas the bottom NES mass is also coupled to the linear structure through essentially nonlinear stiffness element.(Al-Shudeifat, 2014)

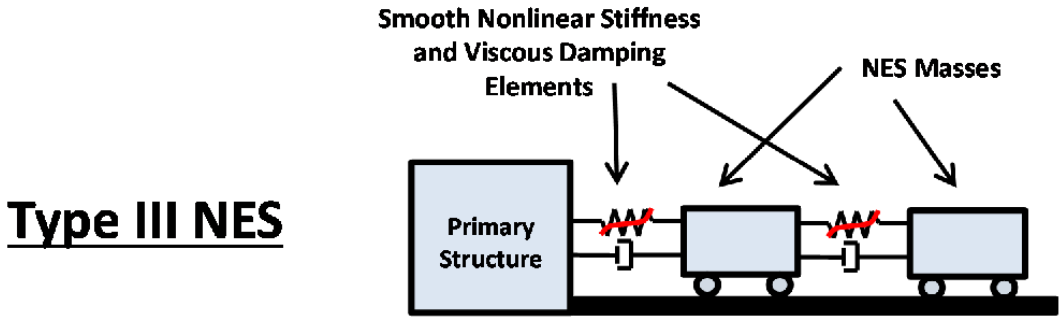

Figure 3 Types of NES (Nicholas E. Wierschem, 2014)

NESs function as DVAs by being attached to critical locations in the primary structure. Their purpose is to passively absorb vibration energy and locally dissipate it through passive targeted energy transfers (TETs). Consequently, energy transfer becomes nearly irreversible, moving from the directly excited primary structure to predefined local attachments (the NESs). These attachments confine and dissipate energy locally without reflecting it back to the primary structure. In this manner, the NESs act as local and adaptive boundary controllers. They can be considered as more

versatile versions of traditional tuned mass dampers, which have a fixed tuned frequency and provide suppression within a narrow bandwidth. Unlike conventional DVAs, NESs offer the following advantages due to their essentially nonlinear spring:

- Implementation of passive targeted energy transfers (TETs).
- Localization and dissipation of energy without backscattering to the primary structure.
- Resonant interaction with multiple structural modes across a wide frequency range.
- Capability to couple structural modes and facilitate energy redistribution from low-frequency modes to high-frequency modes. This allows the structure's intrinsic damping to dissipate energy more rapidly.(Luo, Wierschem, Fahnestock, Spencer, et al., 2014)

Defense Advanced Research Projects Agency (DARPA) Study

In a funded study conducted under the grant of Defense Advanced Research Projects Agency (DARPA), NESs' for vibration mitigation of civil structures were studied using elastomeric bumpers as their essential component for imparting nonlinear stiffness characteristics. The bumpers were realized out of a material with hyper-elastic properties and large scale experimental and computational research was carried out to evaluate the effectiveness of this arrangement.

The study proposed an elastomeric bumper of pyramidal shape that is installed in a device that has sliding mass acting as the mass and damper. The compression effect of the device against the bumper produces the nonlinear stiffness characteristics of the system. The study did the following major undertakings:

- Type I and Type III NESs' were evaluated experimentally on a frame structure using shake table testing.
- Parametric study of geometric features of the elastomeric bumpers were evaluated.
- Finite element analysis for hyper-elastic materials was performed to demonstrate their capability as nonlinear stiffness elements.

This study is directly influenced and motivated by research conducted by (Luo, Wierschem, Hubbard, et al., 2014) and derives its methodologies and objectives from it.

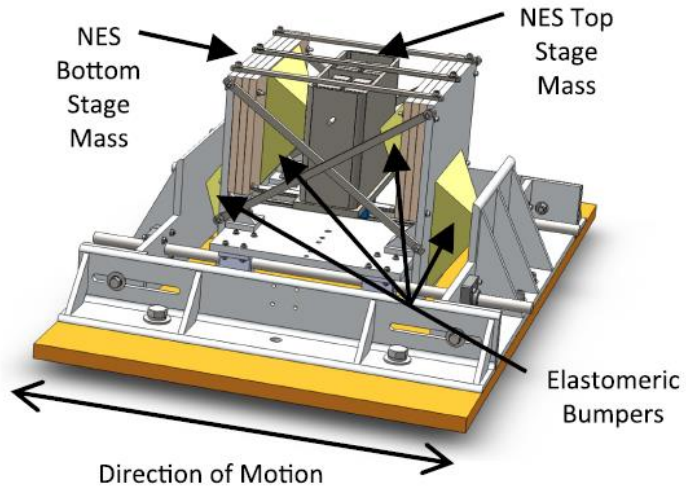

Figure 4 Rendering of Type III NES with Elastomeric Bumpers (Luo, Wierschem, Hubbard, et al., 2014)

Hyper-elastic Materials in Nonlinear Energy Sinks

As proposed by the above study, hyper-elastic materials have the desired characteristics that can be utilized as a nonlinear stiffness element in an NES. Hyper-elastic materials are a category of materials that exhibit nonlinear stress-strain relationships and possess the ability to undergo large deformations without permanent

deformations. They are often referred to as "rubbery" materials due to their high deformability.

Unlike elastic materials, these materials don’t follow Hooke’s law, meaning that the strain magnitude is not directly proportional to the stresses applied and the behavior of material depends on the magnitude and recent history of deformation.

Polyurethanes are a class of polymers that can be formulated with different properties, including hyper-elastic behavior. PU foams are often used for their damping and energy-absorbing capabilities, making them suitable for structural damping applications (Pawlikowski, 2014).

Research Objectives

The primary objective of this study is to conduct a parametric Finite Element Analysis of a Polyurethane Foam in the form of a Truncated Cone geometry to establish the nonlinear stiffness characteristics to be utilized as a nonlinear spring in an NES. A breakdown of the detailed objectives is as follows:

a) Development of a transformable computational model for Essentially Nonlinear Elastomeric Springs for NES
b) Static finite element analysis of hyper-elastic polyurethane elastomer and establishment of its non-linear behavior across load-displacement curve
c) Demonstration of Ogden model for simulating hyperelastic materials under large compressive strains
d) Comparison of change in height of truncated cone shaped polyurethane elastomer on its load displacement curve

e) Demonstration of effectiveness of this type of device in vibration mitigation in civil structures

Methodology

The methodology for achieving the objectives of this study consists of the following steps:

- Static Finite Element Analysis of a hyper-elastic polyurethane is performed in a high-fidelity commercial FEA software **SIMULIA Abaqus FEA**
- A truncated cone geometry is modelled for simulation under compression.
- A parametric study of geometric dimensions is performed, and results are evaluated for Ogden models.
- Finally, the force-displacement curve is imported in ETABS where a sample frame structure story displacement is calculated with and without the NES to evaluate effectiveness.

Problem Statement

The study primarily deals with the finite element analysis of a geometrically nonlinear hyperelastic polyurethane foam up to compressive strains of 80% using Ogden model under compression which can behave as an essentially nonlinear spring in an NES.

Chapter 2: Literature Review

In this chapter, a thorough review of the literature is documented which offers an insight into the vibration mitigation techniques in civil structures, the recent advancements in development of nonlinear energy sinks as a method of vibration mitigation. Then, hyperelastic materials are explored further along with the methods and techniques used in finite element analysis of these materials. A disaster risk profile of Pakistan is also presented which builds on the adoption of the latest international code as Pakistan building code and the necessity it creates for development of advance regimes to make sure new structures comply with the code requirements and the already existing ones can be retrofitted to enhance their response against dynamic forces as per the requirements of the code.

Vibration Mitigation in Civil Structures

Throughout the long history of human presence on Earth, humans have consistently battled against natural perils in order to ensure their survival. Among these perils, earthquakes and powerful winds have posed the greatest challenges when it comes to erecting tall civil structures. These natural forces transmit vibrational energy to these constructions, which typically possess minimal inherent damping capacities (ranging from 0.1 to 5 percent), frequently leading to their collapse. To address this issue and enable the construction of even taller buildings capable of withstanding the forces of nature, extensive research is being conducted on techniques aimed at mitigating vibrations. (El Ouni et al., 2022).

Vibration control systems in civil structures are commonly categorized into passive, active, semi-active, and hybrid techniques for mitigating vibrations. Passive methods

encompass various systems such as tuned mass damper (TMD), tuned liquid damper (TLD), vibration mitigation systems based on inerters like tuned inerter damper (TDI) and tuned mass inerter damper (TMID), as well as structural modifications like top-story softening. Active control techniques involve active tuned mass dampers (ATMD) and piezoelectric actuators. Semi-active approaches comprise negative stiffness devices (NSD), magneto-rheological damper TMD (MR-TMD), and variable stiffness semi-active TMD (VS-STMD). Hybrid systems encompass active base isolation systems and semi-active MR dampers combined with nonlinear base isolators. (El-Khoury & Adeli, 2013).

Passive Vibration Control

Passive vibration control means that no active input requiring energy consumption is required for functioning of the devices as it passively dissipates energy entirely through its damping and stiffness characteristics. A brief review of devices in this category is shown in Figure 5 below.

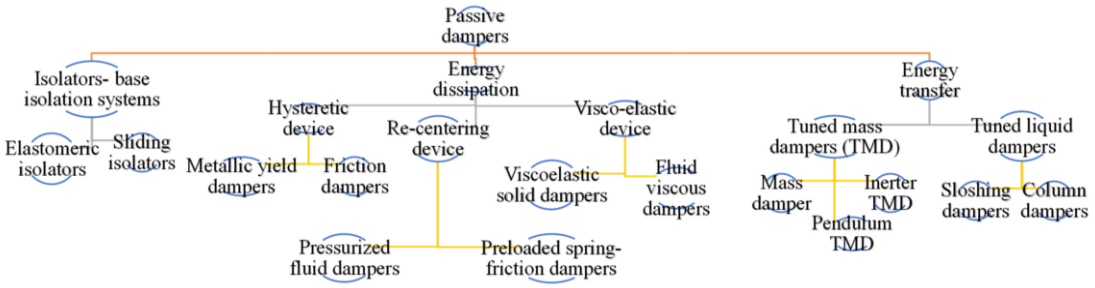

Figure 5 Division for passive damper (El Ouni et al., 2022)

Tuned Mass Damper

Tuned Mass Damping (TMD) is a device used to mitigate vibrations in structures by introducing a secondary mass-spring system. The TMD system is designed in such a way that its natural frequency is very close or equal to the frequency of the structure's

primary vibration. In this way, the TMD can dissipate and absorb the vibrational energy, thereby reducing the amplitude of given structure.

Generally, a tuned mass damping system is implemented like below:

- Primary Vibrational Mode identification
- Tuning Parameters determinations/evaluations
- Configuration of TMD
- Installation and Adjustment
- Absorption and Dissipation of Vibrational Energy

Tuned mass dampers are very useful in structures prone to resonant vibration where the excitation frequency of physical parameters like winds and seismic activity can match the natural frequency of the structure and introduce devastating high amplitude vibrations. In such cases, the TMD acts as a counterbalance and can significantly improve the dynamic response vibrations and their adverse effects. The design and installation of a TMD system require considerations of various factors such as mode shapes and frequency range of interest, not to mention structural characteristics themselves (Elias & Matsagar, 2017).

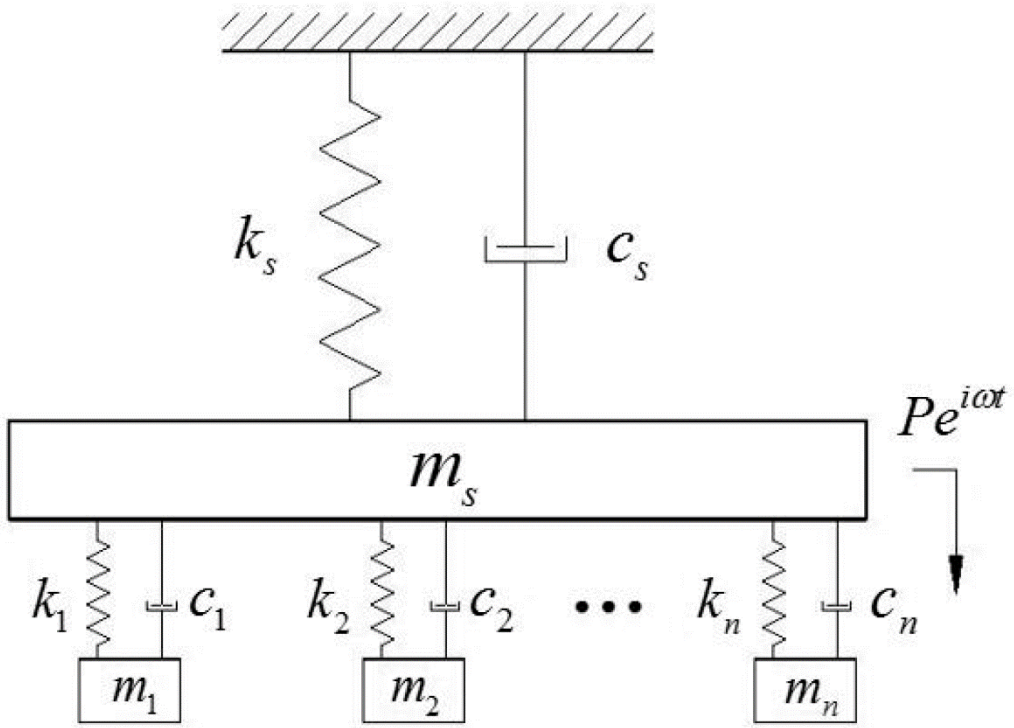

Figure 6 Schematic Representation of Tuned Mass Damper

Tuned Liquid Dampers

The utilization of a Tuned Liquid Damper (TLD) involves harnessing the movement of a partially filled container's shallow liquid (known as sloshing) to effectively decrease the amount of energy caused by vibrations. The shape of the tank and the viscosity of the liquid are deliberately selected to closely correspond to the natural resonance frequency of the structure. By incorporating elements that can dampen the flow such as screens or baffles inside the container, the dissipation of energy from the sloshing liquid can be enhanced. TLDs are available in various container shapes, such as rectangular or circular designs. In contrast to the circular variation, the rectangular type displays two distinct frequencies in two perpendicular directions. For instance, the Shin Yokohama Prince Hotel in Yokohama, Japan, is equipped with tuned liquid dampers. (El Ouni et al., 2022).

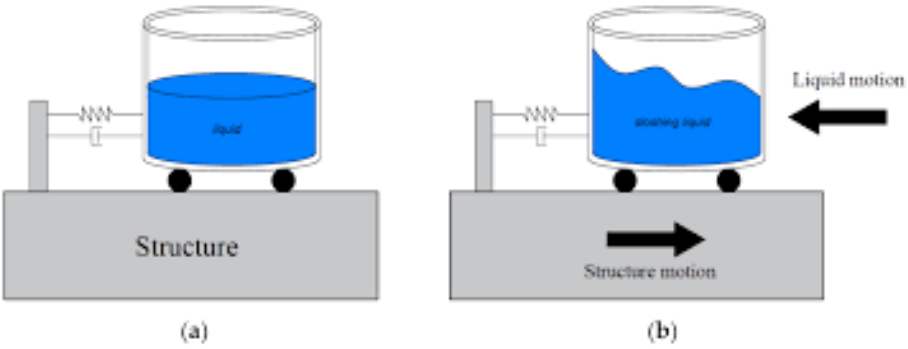

Figure 7 Tuned Liquid Damper Schematic

Tuned Mass Damper Inerter

In the realm of civil engineering for vibration control, an innovative device known as an "inerter" has emerged over the last ten years. This device, referred to as an inerter, generates a force that is directly proportional to the acceleration between its terminals. This force can be likened to a hypothetical mass and is utilized to boost the performance of tuned mass dampers, all without imposing additional vertical loads on building frames. Consequently, this improved device is commonly acknowledged as a tuned mass damper inerter (TMDI). By integrating the inerter with traditional damping devices, further advancements have been made, resulting in the creation of other devices such as the tuned inerter damper (TID), multiple tuned mass damper, and double mass tuned damper inerter (DMTDI).

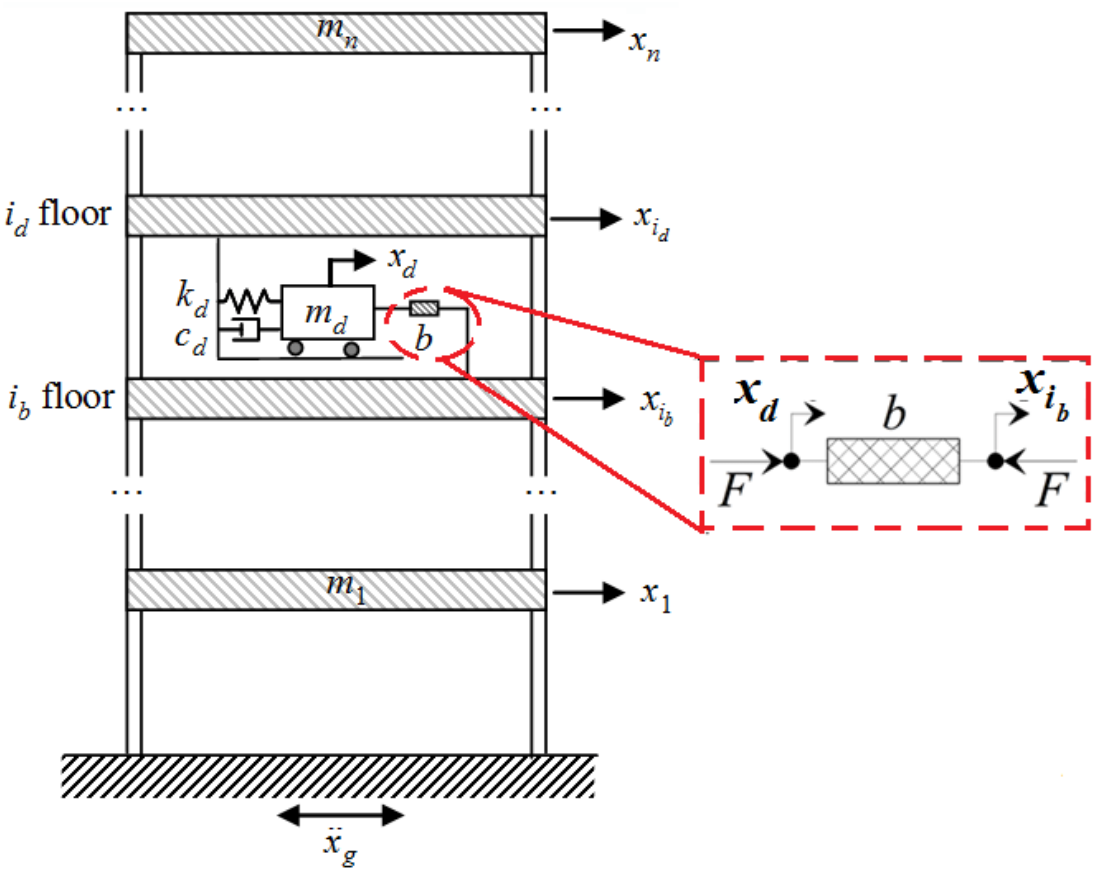

Figure 8 Tuned Mass Damper Inerter Schematic (Agathoklis Giaralis & Alexandros Taflanidis, n.d.)

While there is an increasing interest in utilizing inerter technology within the field of civil engineering, the majority of the research conducted thus far has primarily focused on numerical simulations. Nevertheless, a small number of practical implementations have been witnessed in the context of tall structures. An example of this can be seen in Sendai, Japan, where a building was equipped with a tuned viscous mass damper (TVMD). This system consists of a viscous damper and a ball screw inerter connected in parallel to a spring in series. Its purpose is to enhance the seismic safety of the building by being installed on the upper floors.

Base Isolation Systems

The fundamental principle of isolating the foundations of a building for protection from seismic activity, revolves around the setting up of devices that separate the structure or its main components from potentially dangerous vibrations generated by earthquakes or support movements. This separation is accomplished by increasing the flexibility of the system and implementing appropriate measures to reduce vibration. One commonly used approach is the utilization of laminated rubber (elastomeric) bearing base isolators that could either be with or without lead. Another technique for base isolation involves the application of friction pendulum seismic isolation bearings at each support point, allowing the structure to sway in a gentle pendulum-like motion during ground shaking caused by earthquakes. This enables the ground to shake without causing any harm to the structure. Additional devices employed for base isolation include friction isolation devices, steel energy-absorbing devices that yield under stress, as well as damping devices using visco-elastic and fluid-viscous materials.

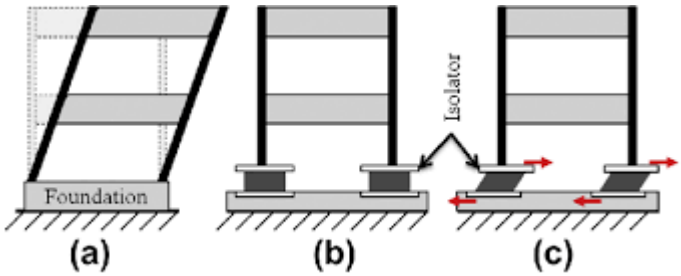

Figure 9 Base Isolation in Civil Structures

Base isolation techniques are commonly applied in mitigating seismic responses for low- to medium-rise buildings. However, there has been a recent proposal to extend the application of base isolation to high-rise buildings. Furthermore, base isolation techniques have been implemented in various real-life structures worldwide.

Numerous buildings have already been isolated, with notable examples including the Utah State Capitol building and Los Angeles City Hall.

Active Vibration Control

This approach employs a collection of interconnected actuators and sensors in a loop that could be forward-feeding or backward-feeding. The figure below illustrates the fundamental configuration of this strategy. In particular, actuators that are based on hydraulic or electromechanical systems and are controlled by an optimizable control algorithm can regulate vibrations in civil structures. This algorithm can be categorized as closed-loop or feedback, where the control forces are determined based on the feedback response of the structure; open-loop or feedforward, where the control forces are determined by measured external excitations; or closed-open loop or feedforward-feedback, where the control forces are determined by both the measured response of the structure and external inputs.

In situations where the parameters of the structure are unknown and require adjustment based on the calculating error between the measured response and the desired response, an adaptive control system can be utilized. This system operates by modifying the closed-open loop control using a controller that is capable of adapting the parameters of the system.

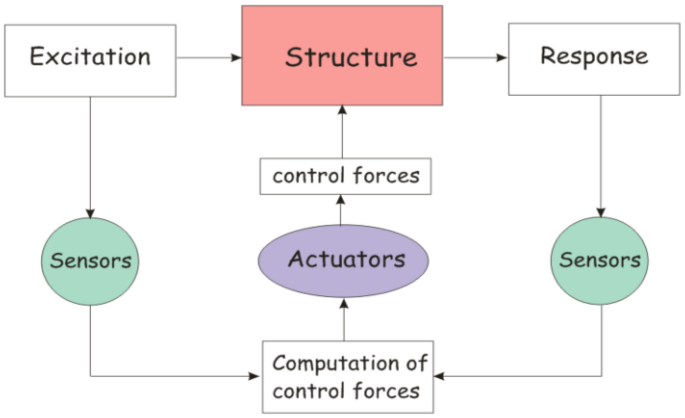

Figure 10 Active Vibration Control Block Diagram

Active Mass Damper

(Abdel-Rohman, 1984) (Samali et al., 1985)

For the Nanjing TV transmission tower in China, (Wu & Yang, 1998). (Yamamoto et al., 2001) (Kobori et al., 1991). (Wang & Lin, 2007). (Guclu & Yazici, 2008).

The Kajima Corporation was the first building in which a full-scale active control system was achieved in 1989, as reported by (Kobori et al., 1991). The Kyobashi Center building was installed with a control system that worked by using two suspended AMDs, with one utilized for transverse motion and the other used to reduce torque or rotational motion. Servo-hydraulic actuators are used to drive the two damper masses (Kareem et al., 1999). According to (Elias et al., 2023), the performance of active controllers for vibration control in buildings subjected to pulse-type or high amplitude repeating ground motions is not substantial, and using assumptions of elastic models is unrealistic.

(Ümütlü et al., 2021) demonstrated the robustness of an adaptive control design for an active TMD system under dynamic forces. They discovered that the proposed system exhibited effective performance in mitigating structural responses, with the absolute instantaneous optimal control performance index being as effective as LQR for an active control system (Yanik, 2019; Yanik et al., 2014).

This approach utilizes an auxiliary mass within an actuator to generate a control force for vibration control, making use of the reaction inertia force as shown in Figure 15. A control computer analyzes the measured response signals and applies a control force based on feedback from the structural response. The actuator then swings or pendulums the secondary mass to counteract the motion of the building. To address vibrations in tall structures, the active mass damper (AMD) was proposed by (Chang & Soong, 1980) in 1980 as an extension of the passive tuned mass damper (TMD). (Abdel-Rohman, 1984) proposed a design procedure for an active TMD to effectively regulate tall buildings subjected to stationary and random wind forces. (Samali et al., 1985) conducted an evaluation of active vibration control in a 40-story building under significant wind excitations using an AMD, comparing the results with a conventional TMD. (Wu & Yang, 1998) put forward an AMD system based on linear-quadratic Gaussian (LQG), H¥, and continuous sliding mode control (SMC) strategies to mitigate vibrations for Nanjing transmission tower China. (Yamamoto et al., 2001) presented the capabilities of AMD systems installed in four actual steel-frame high-rise structures in Japan to mitigate reactions. (Kobori et al., 1991) examined the effectiveness of two AMD systems in controlling torsional and transverse vibrations of a building. A two controller system was proposed by (Wang & Lin, 2007), fuzzy sliding mode control and variable structure control, for buildings equipped with seismic protection and AMD control systems. (Guclu & Yazici, 2008) evaluated the

performance of PD and fuzzy logic controllers for a 15-story frame with AMDs on the top and bottom floors.

Magnetorhoelogical Elastomers

Magnetorheological (MR) materials are smart materials that can change their viscoelastic properties significantly under external stimuli, such as stress, pH level, moisture content, electric fields, or magnetic fields for magnetorheological elastomers (MREs). MREs are especially fascinating materials for actively controlling stiffness and vibration in structural systems. By acting as controllable stiffness elements, MREs provide innovative engineering solutions for various challenges. They are now being used as enabling components in active control systems, such as adaptive tuned vibration absorbers and seismic protection for base-isolated structures.

The response characteristics of MREs depend on several factors, such as the elastomer matrix, the size, distribution, composition, and volume percentage of the ferromagnetic particles, as well as the alignment of these particles in chains or random dispersion. (Ismail et al., 2014) delivers a review of the characteristic properties of magnetorheological elastomers and how these properties are altered by shifting magnetic fields and the specified compositional parameters. In addition to describing the fundamental behavior of MREs, the paper also evaluates and contrasts various applications of MREs for seismic protection.

Nonlinear Devices as DVAs

Nonlinear Energy Sinks

The concept of a Nonlinear Energy Sink (NES) revolves around the development of a nonlinear oscillator devoid of positive linear stiffness. NES possesses the capability to

effectively attenuate vibrations across a wide spectrum of frequencies due to its specific energy transfer properties. Consequently, there has been substantial interest in investigating NES ever since its proposal, with ongoing endeavors to explore its design, analysis, and practical applications for various scenarios.

Over the last twenty years, the exploration of NES, which refers to nonlinear oscillators lacking linear stiffness, has garnered attention due to their inherent ability to passively diminish vibrations. NES is recognized as an intrinsically nonlinear system, rendering linear approximations inadequate for capturing its fundamental dynamic characteristics. An important feature of NES is its capacity to respond across a considerably extensive range of frequencies.

In 2003, the impact of a grounded NES on the steady-state vibration of a linear primary system was examined both theoretically and experimentally. To achieve a cubic nonlinear spring, as depicted in the figure below, an experimental setup utilizing a transversely vibrating steel wire was employed.

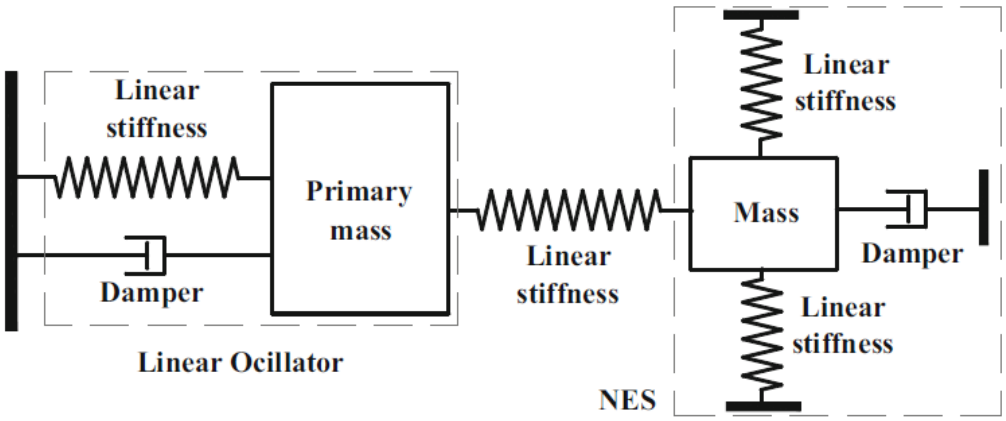

Figure 11 Realization of a Cubic Nonlinear Spring

The remarkable achievement demonstrated the NES's capacity to distribute vibration energy effectively throughout a broad spectrum of frequencies, establishing its superiority over conventional linear vibration absorbers. The research underscored the

crucial role of a non-linear stiffness in maximizing the NES's performance, enabling resonance with all natural modes of the linear system, referred to as the internal resonance condition of 0-m. Notably, it was discovered that a NES with minimal damping could enhance its ability to dissipate vibration energy from the linear system. The equation provided below describes the interaction force F(t) between the primary oscillator and the NES.:

$$F(t) = -k_L(x_P - x_N) - c_N\dot{x}_N - k_N x_N^3$$

Where, k_L represents the coupled linear stiffness.

k_N is the cubic nonlinear stiffness coefficient provided by the vertical springs. c_N is the NES damping coefficient.

x_P and x_N denote the displacements of the primary mass and the mass of the NES, respectively.

Designs of NES

Utilizing the design configuration outlined in (McFarland et al., 2005), a proactive strategy of employing a symmetric design approach has been adopted to attain nonlinear stiffness within Nonlinear Energy Sinks (NES). In order to incorporate cubic nonlinearity, (Gourdon et al., 2007) conducted experimental implementations employing two linear springs. The accompanying mechanical schematic of their arrangement is depicted in the figure provided below.

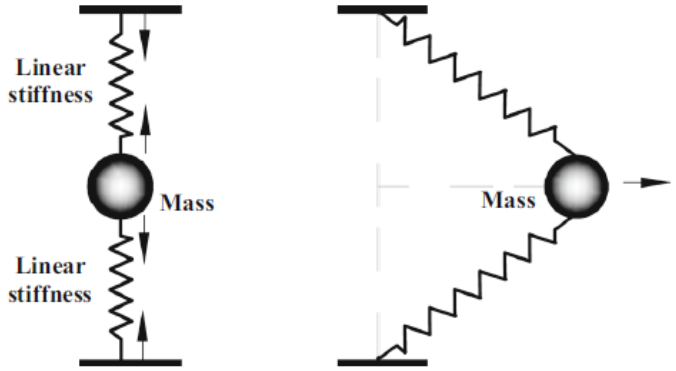

Figure 12 Cubic Nonlinearity Using 2 Springs

Vibro-impact NESs

(GEORGIADIS et al., 2005) A shock isolator was created using two Nonlinear Energy Sinks (NESs) integrated with non-smooth nonlinear stiffness components. The effectiveness of this shock isolator in quickly dissipating a large amount of unwanted shock energy was shown. The use of both smooth and non-smooth stiffness nonlinearities in the design of the NESs exploits the promising capability of vibro-impact nonlinearities for fast passive energy dissipation through focused energy transfer on a rapid timescale.

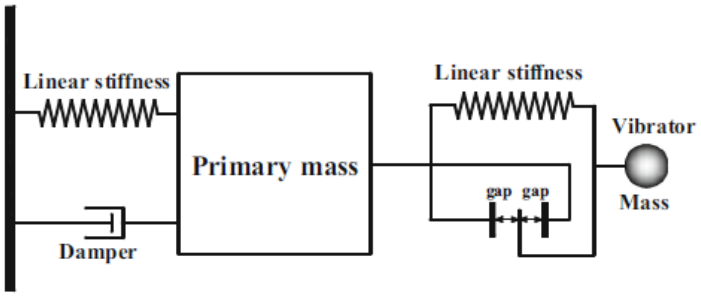

Figure 13 Vibroimpact NES Schematic

NESs with nonlinear damping

(Andersen et al., 2012)presented a Nonlinear Energy Sink (NES) featuring geometrically nonlinear viscous damping.

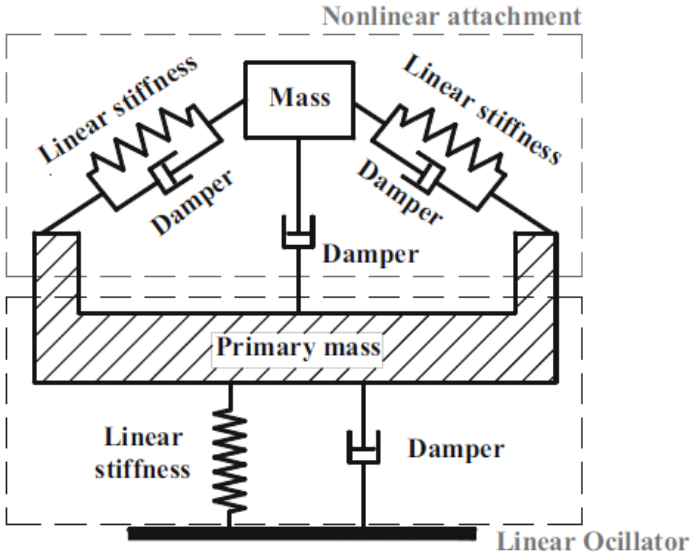

Figure 14 NES with Nonlinear Damping

Multi-DOF NESs

Single-degree-of-freedom (DOF) Nonlinear Energy Sinks (NESs) offer a wider frequency range for dampening vibrations and reducing shocks compared to linear vibration absorbers. However, it should be noted that a single-DOF NES is sensitive to variations in external forcing magnitude and overall energy levels (Raze & Kerschen, 2020). pecifically, it efficiently transfers targeted energy within a relatively narrow range of external forcing amplitudes. In order to overcome this limitation, researchers have investigated passive targeted energy transfer from a linear discrete system of interconnected oscillators to a multi-DOF NES (*Nonlinear Targeted Energy Transfer in Mechanical and Structural Systems*, 2009). Figure below shows the two-DOF NES proposed by (Benarous & Gendelman, 2016) which consists of a purely cubic oscillator and an internal rotator. A comparison between the two-DOF NES and a single-DOF NES of equal weight demonstrated the superiority of the two-DOF NES across all energy ranges beyond the excitation threshold.

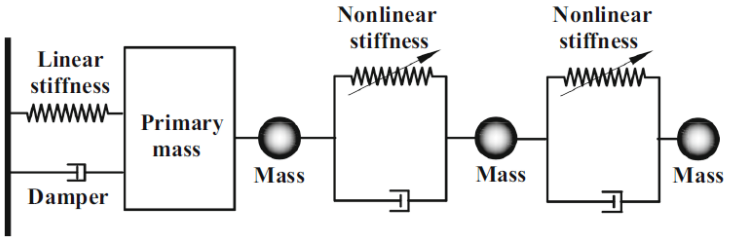

Figure 15 Multi-Degree of Freedom NES

Bi-stable NESs

(Al-Shudeifat, 2014) The snap-through configuration with geometric nonlinearity was employed to aggressively create a bi-stable Nonlinear Energy Sink (NES), as shown in the accompanying figure.

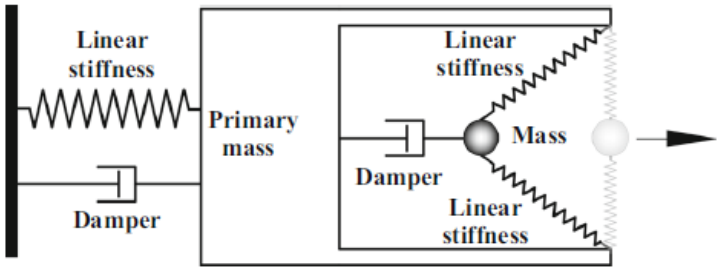

Figure 16 Bi-Stable NES

Figure above displays the Bi-Stable NES, where two linear springs (depicted in black) play a crucial role. These springs have the ability to generate both negative linear and positive nonlinear stiffness terms as the NES mass moves. By incorporating the bi-stable NES, a remarkable improvement is achieved in terms of targeted vibration energy transfer and fast local energy dissipation. Remarkably, when exposed to a wide range of initial energy and with the NES mass strategically positioned relative to the primary mass, the bi-stable NES was able to dissipate an astonishing 97-99% of the input energy originating from the primary oscillator.

Summary

Nonlinear Energy Sinks (NESs) have emerged as effective tools for mitigating structural vibrations. They offer several advantages over traditional linear vibration absorbers, including a wider frequency band for vibration suppression and the ability to efficiently transfer and dissipate energy. NESs' utilize controlled nonlinearities, such as nonlinear stiffness or geometric configurations, to absorb and dissipate vibrational energy.

Various types of NESs have been investigated, including single-degree-of-freedom (DOF) NESs, multi-DOF NESs, bi-stable NESs, and NESs with geometrically nonlinear damping. These configurations have been designed to enhance targeted energy transfer, improve performance across a broader range of external forcing amplitudes, and increase local energy dissipation.

Applications of NESs in structural vibration mitigation include shock isolation, seismic protection, and reducing vibrations in tall buildings and other structures. They have shown promise in effectively suppressing vibrations, mitigating shock loads, and improving the overall dynamic response of structures. Research efforts continue to explore new designs, analysis methods, and practical applications of NESs for different engineering challenges.

In summary, NESs offer innovative solutions for structural vibration mitigation by harnessing nonlinear energy transfer and dissipation mechanisms. Their unique characteristics make them a promising approach to enhance the resilience and performance of structures subjected to dynamic loads.

Types of Hyper-elastic Materials Suitable for Vibration Damping

Hyper-elastic materials can be categorized into various classes based on their specific material properties and chemical composition. Some categories of hyper-elastic materials include:

1. Elastomers: Elastomers are a class of hyper-elastic materials characterized by their high deformability and ability to return to their original shape after deformation. These materials exhibit significant elasticity and are widely used in applications requiring flexibility and resilience. Natural rubber and various synthetic rubbers, such as silicone rubber and neoprene, are examples of elastomers (Kadlowec et al., 2003).

2. Polyurethanes (PU): Polyurethanes are a class of polymers that can be formulated with different properties, including hyper-elastic behavior. PU foams are often used for their damping and energy-absorbing capabilities, making them suitable for structural damping applications (Pawlikowski, 2014).

3. Magnetorheological Elastomers: Magnetorheological elastomers (MREs) are a type of smart material that combines the characteristics of elastomers with the controllable rheological properties of magnetorheological fluids. MREs exhibit the ability to undergo large deformations and simultaneously change their mechanical properties under the influence of a magnetic field (Kang et al., 2020).

4. Thermoplastic Elastomers (TPE): Thermoplastic elastomers combine the characteristics of rubber-like elasticity with the processability of thermoplastics. They offer good mechanical properties and can be easily molded and shaped. TPEs are used in various industries, including automotive, consumer goods, and medical devices (Qi & Boyce, n.d.).

5. Micro-/Nanostructured Mechanical Metamaterials: The concept of metamaterials as per (Lee et al., 2012) were first introduced in the field of electromagnetic (EM) materials. It is a material whose effective properties arose not from the bulk behavior of the materials which composed it, but more from their deliberate structuring. These materials can be designed and fabricated to exhibit properties that are generally not the characteristic of natural materials, for example, negative Poisson's ratio etc.

Hyper-elastic Simulation Models

There are various classes of hyperelastic materials based on their models and mathematical descriptions. Some of the categories are:

a) Neo-Hookean Model: The neo-Hookean model assumes that the stored energy in the material is solely determined by its current deformation state and is independent of its previous history. This model is based on the assumption of incompressibility and is mathematically described using the strain energy density function.

b) Yeoh hyperelastic model: An improvement over the neo-Hookean model, The Yeoh model incorporates higher-order non-linear terms to better capture the material behavior under larger strains. It is most suitable for small deformations or low-strain regimes. It is capable of capturing non-linear material behavior at larger strains. It is more versatile and applicable to wider scenario ranges. The reduced polynomial form based on first strain invariants of the right Cauchy-Green tensor only is the well known Yeoh model, which is commonly considered with N=3 (Huri & Mankovits, 2018)

$$W = \sum_{i+j=1}^{N} c_{i0} (\bar{I_1} - 3)^i + \sum_{k=1}^{N} \frac{1}{d_k} (J - 1)^{2k}$$

c) Arruda-Boyce Model: The Arruda-Boyce model is specifically designed for compressible hyperelastic materials and takes into account the volumetric response of the material. It is commonly used for rubber-like materials.

d) Mooney-Rivlin Model: The Mooney-Rivlin model is an extension of the neo-Hookean model and considers additional strain energy terms. It offers a more accurate representation of the material behavior for large deformation cases. The Mooney-Rivlin model uses material parameters to describe the non-linear response of the material. In finite elasticity, the Mooney–Rivlin material model for the Cauchy stress tensor T in terms of the left Cauchy–Green strain tensor B is given by

$$T = -pI + s_1 B + s_2 B^{-1}$$

Where, p is the pressure, and s_1, s_2 are two material constants.

It is usually assumed that $s_1 > 0$ and $s_2 \leq 0$, known as E-inequalities, based on the assumption that the free energy function be positive definite for any deformation(Liu, 2012).

e) Fung Model: The Fung model is a hyperelastic material model used for soft biological tissues. It incorporates an exponential strain energy function and captures the anisotropic behavior of biological tissues.

f) Ogden Model: The Ogden model is a more general hyperelastic model that allows for a wide range of material behaviors. It is based on the concept of strain energy density function and can accurately represent various deformation characteristics, such as strain stiffening or softening.

Experimental and Numerical Studies

The success of a finite element simulation of rubber components depends heavily on the careful selection of a suitable strain energy function and the accurate determination of material constants. Due to the intrinsic incompressibility of the material, the strain energy function can be divided into separate components (Huri & Mankovits, 2018)

$$W = W_D(\bar{I_1}, \bar{I_2}) + W_b(J)$$

Where, $W_b(J)$ denotes the volumetric terms of the strain energy function.

J is for the Jacobian

$W_D(I_1, I_2)$ is for the deviatoric terms of the strain energy function

The polynomial form of the strain energy potential is based on the first I_1 and second I_2 strain invariants of the right Cauchy-Green tensor.

$$W = \sum_{i+j=1}^{N} c_{ij} (\bar{I_1} - 3)^i (\bar{I_2} - 3)^j + \sum_{k=1}^{N} \frac{1}{d_k} (J-1)^{2k}$$

where determination of c_{ij} and d_k material constants are required in material model. The κ bulk modulus can be calculated as

$$\kappa = \frac{2}{d}$$

where d is the material compressibility parameter.

There have been numerous studies exploring various hyperelastic materials and their use in structural damping according to their applicability(Huri & Mankovits, 2018).

Elastomer Material

The use of elastomer materials with Yeoh hyperelastic model (Gajewski et al., 2015) discusses the benefits of using it over the simpler non-Hookean model in the following steps:

- Constitutive modeling of elastomeric bearings components
- hyperelasticity parameters determination
- Conducting compression and shear tests of elastomeric bridge bearing

The study concludes that Yeoh model is more accurate in predicting the damping properties of an elastomer, however, the viscous properties (discusses further ahead) are also to be kept in mind while testing a damper.

Polyurethane Elastomer

The next study for (Sheikhi et al., 2021) polyurethane elastomer explores the use of the following material models to acquire stress-strain relations and curve fitting of data for determining the material constants.

- Mooney–Rivlin
- Ogden

- Neo-Hookean
- Gent

The ANSYS software was employed to input the data and perform additional simulations, producing the following outcomes:

- The Gent model emerged as the most superior material model for uni-axial tension testing.
- The uni-axial stress + bi-axial data set has been shown as the optimal combination for numerical analysis of materials subjected to uni-axial tension testing.
- When it comes to pure shear testing, the neo-Hookean model has proven to be the most effective material model.

Magnetorheological Elastomers

Another study (Kang et al., 2020) tracks the characteristics and applicability of Magnetorheological (MR) elastomers which are a promising new sector of elastomers.

The fabrication of these materials involves adding CIP's powder along with catalyst to make a sample and using magnetic flux in vacuum conditions to align the soft-magnetic particles inside the elastomer while it cures into a solid. The techniques are used for isotropic and anisotropic MREs are slightly different due to nature of materials.

The sample material undergoes testing that determines its tensile properties, damping loss factor and magnetic properties. MREs can be used for multiple applications like

- Vibration Absorber
- Vibration Isolator
- Magnetoresistor Sensor
- Electromagnetic Wave Absorber

These MREs have the added benefit of being able to utilize waste rubber, thereby, reducing the carbon footprint of the cycle.

Micro-/Nanostructured Mechanical Metamaterials

The use of Nanostructured Mechanical Metamaterials for vibration damping as studied by (Lee et al., 2012) also show an exciting new family of materials that can be utilized for vibration damping applications. The study discusses the Characteristics of the MNSMs including their static modulus, specific energy absorption and heat transport etc. It also investigates various manufacturing techniques that can be applied towards fabrication of MNSMs and the resulting characterization of materials acquired via these techniques.

Their study shows that such structures with sufficiently small lattice constants will enable metamaterials for high frequency applications and despite the challenges in the way of sustainable manufacturing, these metamaterials show promise into future applications.

Future Directions and Challenges

The future of hyperelastic materials in vibration damping shows promise towards improved materials and more efficient applications.

Regarding materials, it is inevitable from the resources used to conduct this study, that Smart materials are the most promising aspect. They are however, not without current limitations, and any study or research directed towards the environment friendly and sustainable manufacturing of such materials is sure to yield fruitful results.

The high costs of soft-magnetizing and the difficulties faced in internal structuring of Mechanical Metamaterials also proves a challenge that scientist and engineers are working on and is sure to show significant advances in the near future.

Chapter 3: Finite Element Analysis of Hyper-elastic Material – Computational Framework

This chapter is a detailed documentation of the steps followed in computational simulation of hyper-elastic polyurethane material using SIMULIA Abaqus FEA. First, it briefly describes the various steps of an FEA analysis. Then it states step by step, the implementation of these steps in this study and the tradeoffs associated with them. Finally, it argues about the validity of the results achieved.

Finite Element Analysis

FEA is a useful computational tool developed to analyse and evaluate complex engineering problems, primarily in structural mechanical and aerospace divisions of engineering. It has revolutionized the approach engineers use to design and optimize systems by giving insight to their behavior under various conditions.

FEA is primarily based on dividing a geometry or system into smaller discretized elements which combine to form a mesh of interconnected elements. A set of nodes are then assigned to each element by the software and the behavior of the entire system is approximated by producing a solution of the governing equations at these nodes. FEA is a versatile tool providing acceptable solutions to a wide range of engineering problems. FEA also comes with a number of challenges such as construction of a reliable and predictive mesh, element geometry, material selections and suitable boundary conditions.

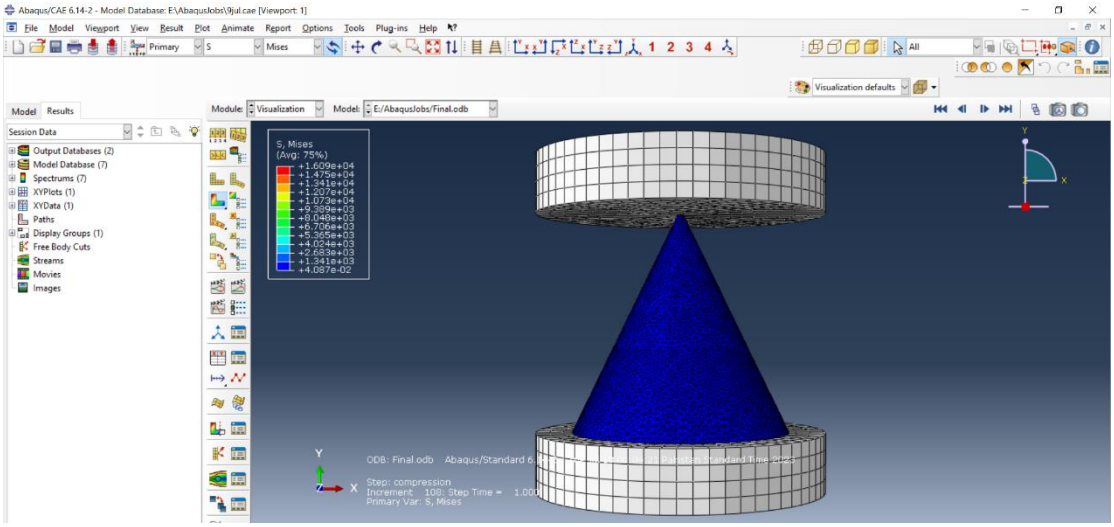

Figure 17 Cone in Compressive Setup - Initial

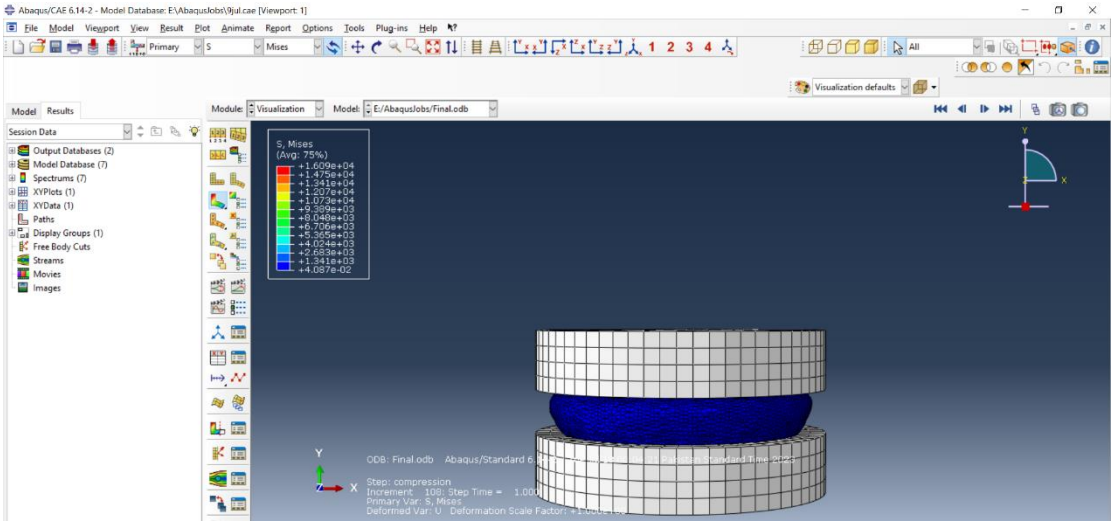

Figure 18 Cone in Compressive Setup - Final

Software and Steps

SIMULIA ABAQUS CAE is a widely utilized software for finite element analysis and the same is used for our analysis. A typical finite element analysis consists of the following steps:

1) Define the Geometry.
2) Define Material Properties.

3) Material Model Selection.
4) Apply Boundary Conditions.
5) Discretization.
6) Problem Solution using Computational Resources.
7) Post-processing.

Defining the Geometry

International standards like ASTM D 3574 (*Standard Test Methods for Rubber Properties in Compression 1 2. Referenced Documents 2.1 ASTM Standards: D 3183 Practice for Rubber-Preparation of Pieces for Test Purposes from Products 2 D 3767 Practice for Rubber-Measurement of Dimen-Sions 2 D 4483 Practice for Determining Precision for Test Method Standards in the Rubber and Carbon Black Industries 2 E 4 Practices for Force Verification of Testing Machines 3*, n.d.) specifies the dimensions and compression rates for determining the material properties of hyper-elastic rubber like materials. While in the study referenced in the introduction chapter, of this document used a pyramidal shaped specimen to enhance the non-linearity of force-displacement. Pyramid shape has the inherent disadvantage of stress concentration due to sudden change in geometry (*Stress Concentration*, n.d.). Moreover, computational resources required to simulate this geometry are much more compared to a geometry with little to no stress concentration. In light of these facts, a truncated cone geometry was selected to demonstrate the hyper-elastic compression. It has the following advantages:

- Geometric stress concentration factors are eliminated.

- A truncated geometry ensures that the contact with he compression surface ensures a more evenly divided stress Therefore, the geometric characteristics of our specimen are documented in the table and shown in the figures below:

Table 1 Geometric Characteristics of Cone

Geometric Characteristics of Truncated Cone Specimen		
Base Diameter (mm)	Top Diameter (mm)	Height (mm)
75	02	75

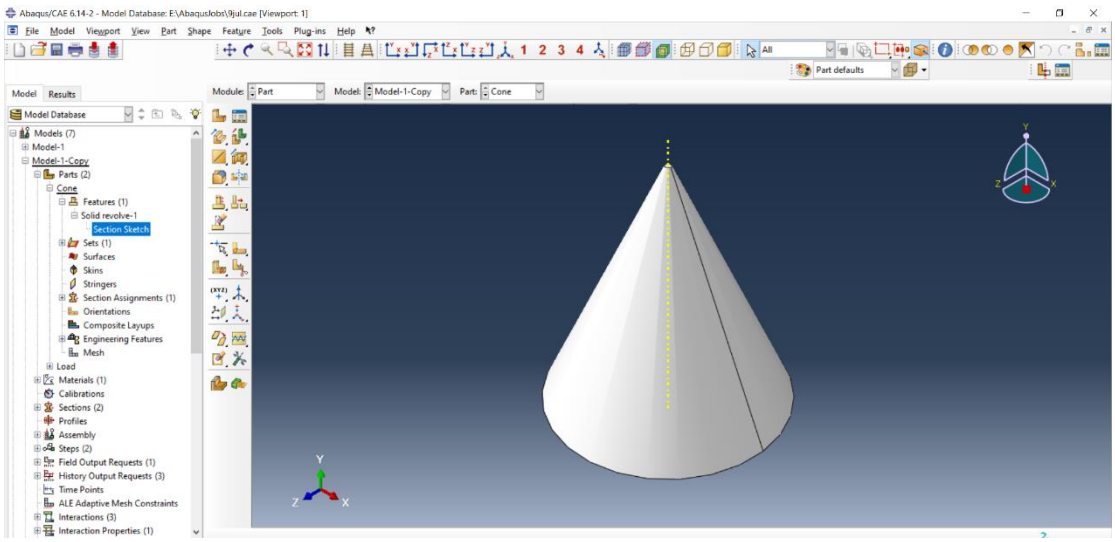

Figure 19 Truncated Cone

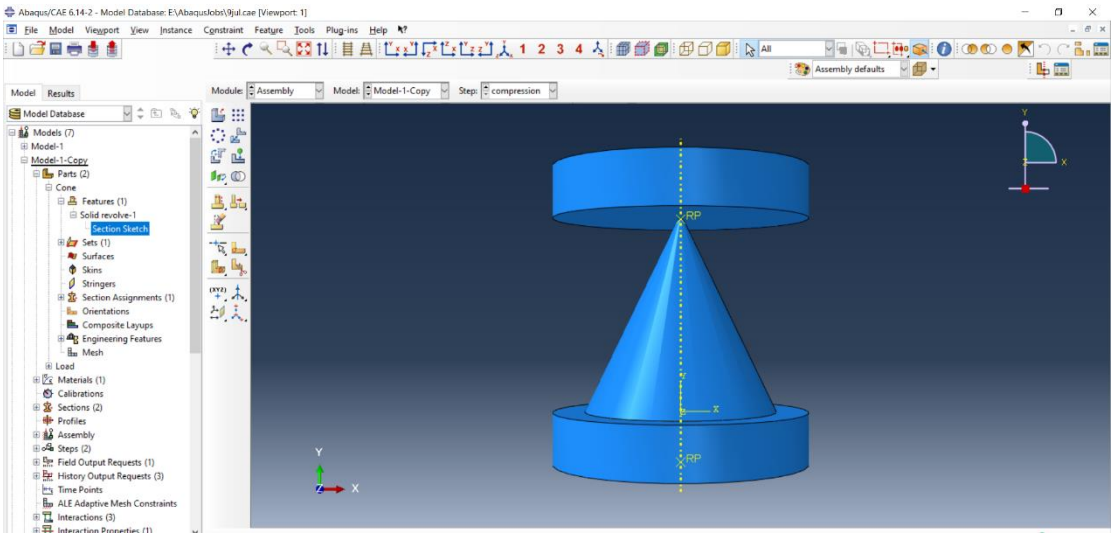

Figure 20 Final Assembly

Defining Material Properties

Polyurethane foam is characterized by its lightweight nature, low stiffness, exceptional insulation capabilities, a decreased Poisson ratio, reduced density (below 80 kg m^3 for flexible foam), high compressibility, slow recovery rate, and its capacity to efficiently absorb strain energy. (Ju et al., 2015). The main reason for choosing this material is the establishment of its hyper-elastic material models through a robust study undertaken as per the standards defined in ASTM D 3574.

Hyper-elastic material models are usually backed with extensive experimental data. In absence of an experimental facility, reliance on an already accepted study was the most sensible course of action to ensure the validity of this simulation. Detailed material properties are documented in the table below.

Table 2 Properties of Polyurethane

Chemical and Morphological Properties of Polyurethane Hyperelastic Foam	
Foam Type	Flexible Polyurethane Foam
Isocynate	Toluene diisocynate TDI
Polyol	Polyether
Expansion Gas	CO_2
Fabrication Process	Free Rise
Density	47 kg/m^3
Cell Population Density	3.27 /mm2
Density Standard Deviation	0.84 kg/m^3
Average Cell Size	457 µm
Sample Shape	Cubic
Dimensions (L x W x H)	75mm x 75mm x 75mm

The material was experimentally tested by (Ju et al., 2015) for determining its stress-strain curve under compression and that data was used to determine the hyper-elastic model parameters. These parameters are further discussed in the material model selection.

Material Model Selection

Hyperelastic constitutive laws are commonly used for modeling materials that show elastic behavior under extremely high levels of deformation. In the theory of hyperelasticity, a strain energy function is present, designated as such.:

$$W = W(F) \; or \; W = W(\lambda_1, \lambda_2, \lambda_3)$$

where F is the deformation tensor, where λ_i (i=1.2.3) are the principal stretches and are given by

$$\lambda_i = 1 + \varepsilon_i$$

where ε_i are strains (for compression $\varepsilon_i < 0$) to describe the hyperelastic phenomenon. The strain energy functions with principal stretches are used and the stress can be derived from the function by

$$\sigma_i = \frac{\lambda_i}{J}\frac{\partial W}{\partial \lambda_i}$$

where J is the determinant of the deformation gradient

The hyperelastic model developed by Ogden is widely used for compressible materials and the stored energy, W, is expressed in the form of a series:

$$W = \sum_{n=1}^{N} \frac{\mu_n}{\alpha_n}\left(\lambda_1^{\alpha_n} + \lambda_2^{\alpha_n} + \lambda_3^{\alpha_n} - 3\right) + F(J)$$

where μ_n, α_n are material parameters, F(J) is the volumetric function.(Ju et al., 2015)

The Ogden model parameters determined from the experimental study for the given model are:

Table 3 Ogden Parameters

Ogden Parameters for Strain Energy Potential Order N = 3					
μ_1	α_1	μ_2	α_2	μ_3	α_3
10.54	1.88	-10.53	1.87	0.00024	27.62

This model was established to be able to simulate the material behavior under compression with an error of 3.33% up to strains of $\varepsilon = 0.8$ or 80% (Ju et al., 2015)

Boundary Conditions and Loading

A discrete rigid shell element of diameter 100mm is modeled to apply compressive load to the geometry under study. An instance of this element is placed in connection with the bottom of the elastomer, and another is placed at the top.

- The one at the bottom of the elastomer is constrained with encaster (X=0, Y=0, Z=0, MX=0, MY=0, MZ=0) boundary condition which restricts its translational and rotational movement in all directions.
- The one at the top is imparted a displacement regime that compresses the elastomer to the desired range (80% strain) for this study.

Meshing and Discretization

Hyperelastic materials in ABAQUS are meshed using Linear, Tetrahedral Hybrid or Plane Stress elements. (Luo, Wierschem, Fahnestock, Spencer, et al., 2014) uses tetrahedral elements in hybrid formulation for the simulation of hyperelastic pyramid

under compression. These mesh elements can capture the large deformation behavior fairly accurately. In our study, we use:

- C3D4H a 3D, 4-node, linear tetrahedral element with hybrid formulation
- C3D10I a 3D, 10-node, linear tetrahedral element

In Abaqus, C3D4H and C3D10I are both element types commonly used in finite element analysis (FEA) for three-dimensional simulations. These elements are part of the continuum element family and are widely employed for various engineering applications.

C3D4H:

The C3D4H element is a 3D, 4-node, linear tetrahedral element with hybrid formulation. It is sometimes referred to as the hybrid solid element. This element combines the advantages of reduced integration and selective reduced integration techniques, aiming to provide accurate results for a wide range of problems.

Key features of the C3D4H element:

Quadratic deformation behavior: Although the element has 4 nodes, it provides quadratic interpolation, allowing for more accurate representation of the displacement field compared to a linear element.

Hourglass control: The C3D4H element includes hourglass control mechanisms to suppress the spurious hourglass mode. "Hourglass control" in Abaqus refers to a technique used in finite element analysis to minimize or control the development of hourglass deformations during the simulation. Hourglass deformations are non-

physical, parasitic, and often unwanted oscillations that can occur in some finite element models, particularly when using reduced integration elements.

Reduced integration elements have fewer integration points than their higher-order counterparts, which can lead to spurious, zero-energy modes, like hourglass modes. These modes can cause artificial distortions and inaccurate results in the analysis. Hourglass control aims to suppress or limit these modes by introducing additional forces or constraints. which can cause instability and numerical artifacts in the analysis results.

Good performance: It is commonly used for solid mechanics simulations and can accurately capture deformation, stress distribution, and other mechanical properties.

C3D10I:

The C3D10I element is a 3D, 10-node, linear tetrahedral element. It is also known as the incompatible mode element. This element type provides linear interpolation of displacements and quadratic interpolation of incompatible modes, allowing for enhanced accuracy in capturing complex deformation patterns.

Key features of the C3D10I element:

Enhanced deformation representation: With 10 nodes, the C3D10I element offers more degrees of freedom, enabling improved deformation representation and the ability to handle complex geometries and loading conditions.

Incompatible modes: The element includes additional degrees of freedom known as incompatible modes, which allow for capturing incompressibility, volumetric locking, and other complex deformation phenomena more accurately.

Suitable for nearly incompressible materials: The C3D10I element is particularly useful when analyzing materials with nearly incompressible behavior, as it effectively mitigates the volumetric locking issue associated with standard solid elements.

Both the C3D4H and C3D10I elements have their own strengths and are employed in different scenarios based on the requirements of the analysis. The selection of the appropriate element type depends on factors such as the material behavior, geometry, and accuracy requirements of the simulation.

The final mesh data is tabulated below:

Table 4 Mesh Data

Mesh Data	
No of Elements	131074
No of Elements defined by user	101114
No of Internal Elements Generated	29958
No of Nodes	100130
No of Nodes defined by user	21227
No of internally generated nodes	78903
Total No of Variables in the Model	172548

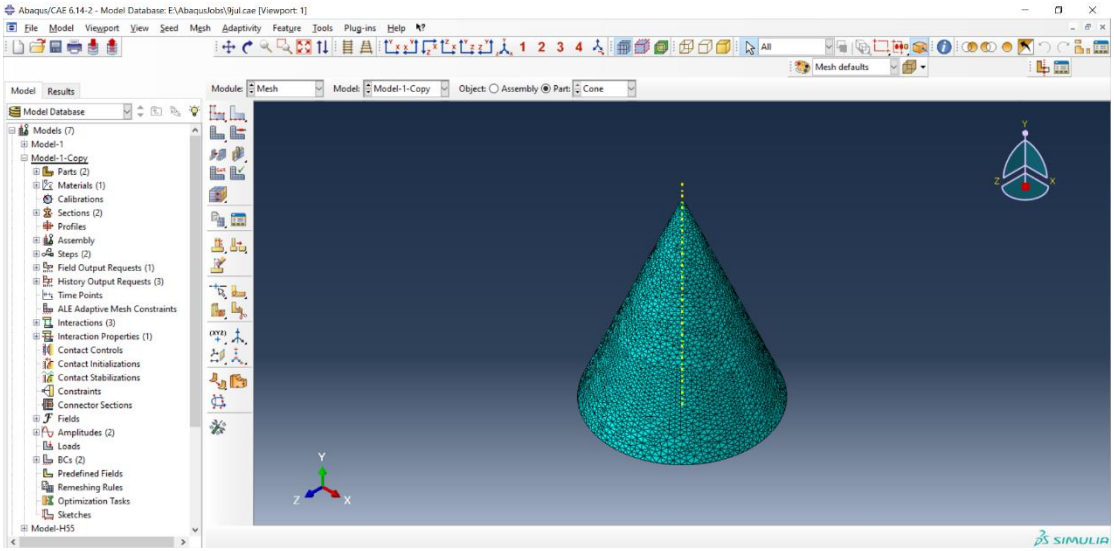

Figure 21 Meshed Cone

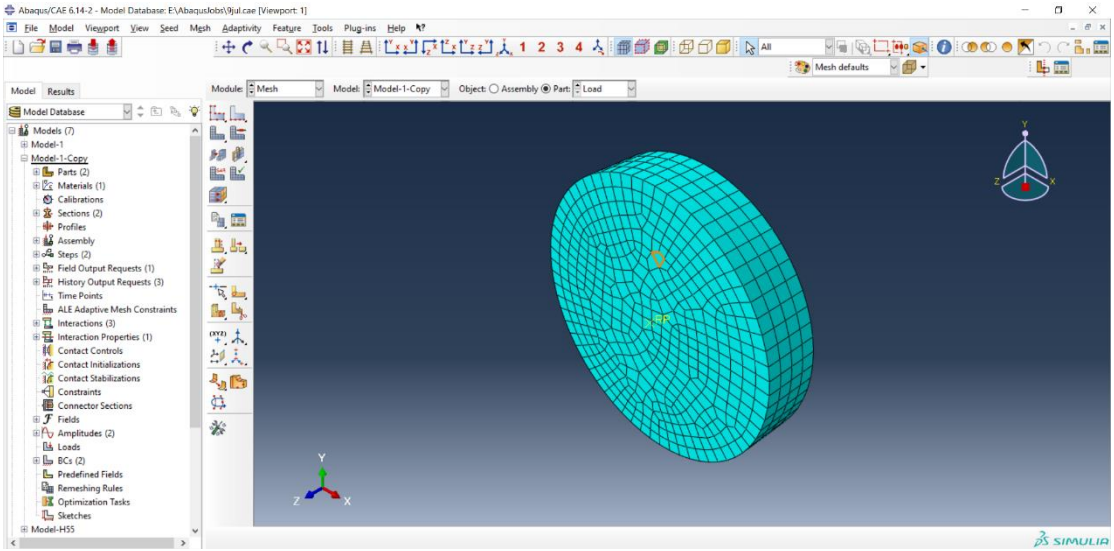

Figure 22 Meshed Shell Element for Loading

Problem Solution using Computational Resources

This part is handled using available computational resources and obviously, a computationally demanding problem like simulation of hyperelastic material under compression is computationally demanding in nature. The PC used for solving the problem had the following specifications:

Table 5 PC Specifications

PC Specifications	
Processor	Intel(R) Core(TM) i7-7700HQ CPU @ 2.80GHz 2.81 GHz
Installed RAM	12 GB
GPU	NVIDIA GeForce GTX 1050Ti with 4GB GDDR5 Ram
OS	Microsoft Windows 10, 64-bit OS

Although the PC was able to handle the problem to a working resolution, a more powerful computational resource could have produced more accurate and precise results.

Post-Processing

Post-processing of the simulation is done by extracting the force-displacement and the stress-strain curves for the compression simulation using ABAQUS post-processing module. The specimen under initial unloaded and final fully loaded conditions is represented in the figures below. The graphs are tabulated and discussed in the next chapter.

Chapter 4: Results and Discussions

In this chapter, a detailed discussion on the results of the simulation described in the previous chapter is presented. The force-displacement and stress-strain graphs are plotted to study the behavior of elastomeric material. A parametric comparison for specimens of different heights is done to plot a trend and finally, the effectiveness of the NES employing this elastomer is demonstrated through a representative frame structure in ETABS.

Hyper-Elastic Material Behavior under Compression

The Following graphs tabulated below are representative of the hyperelastic material behavior under compressive loading.

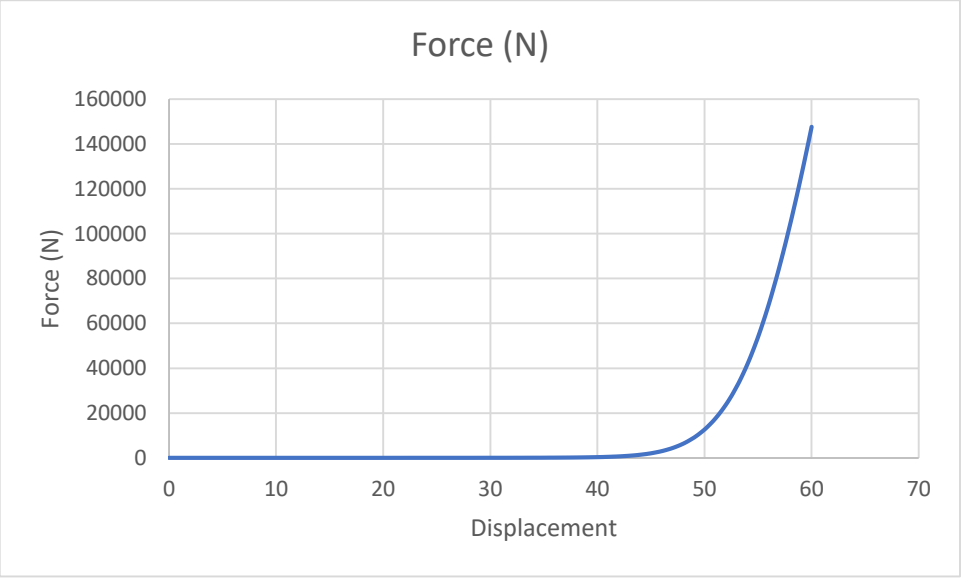

Figure 23 Force-Displacement Graph for 60 mm Displacement

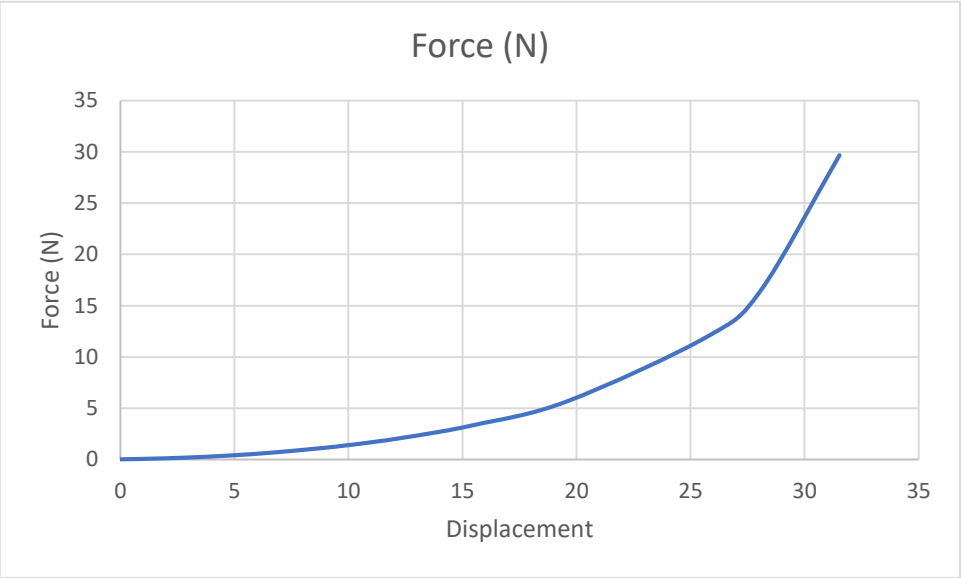

Figure 24 Force-Displacement Graph for 30mm Displacement

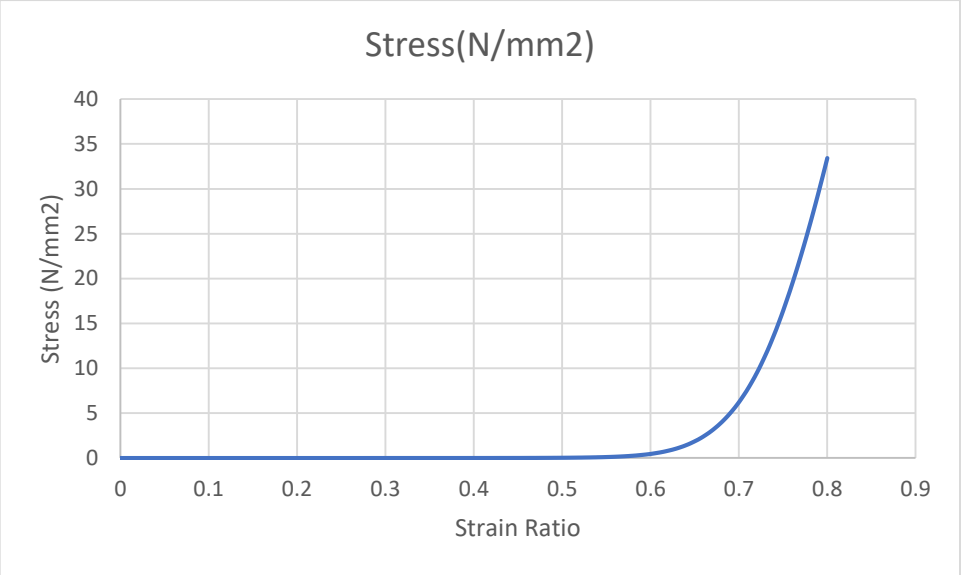

Figure 25 Stress-Strain Graph for 80% Strain

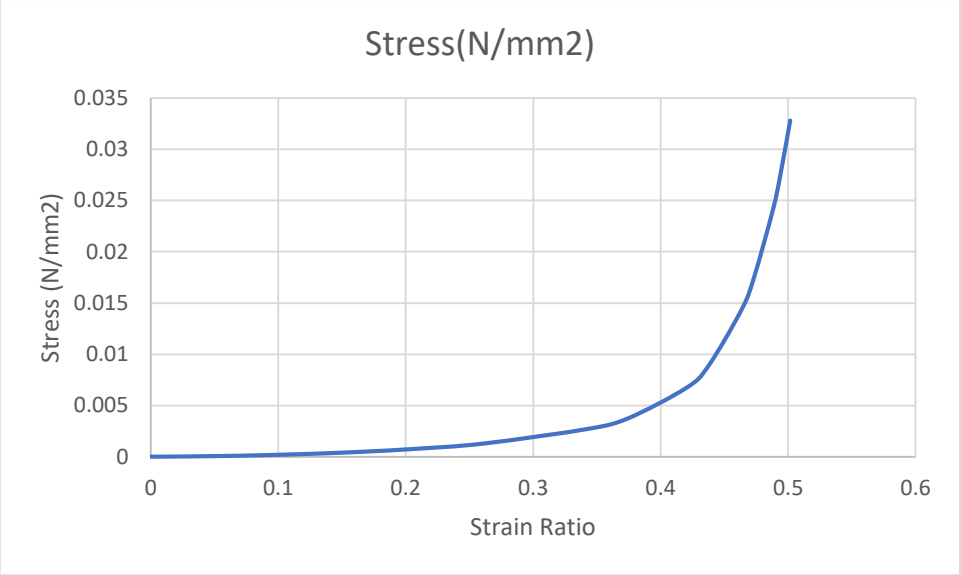

Figure 26 Stress-Strain Graph for 50% Strain

From the above displayed graphs, following results can be concluded:

1) The specimen exhibits strongly non-linear behavior as evident in its force-displacement and stress-strain curves.
2) Although it seems like the stress is negligible for the initial part of compressive strain, by plotting another graph up to approximately 50% strain, we can see that the non-linear behavior is evident in this part of the curve as well.
3) The stresses generated after 70% compression are much more pronounced than before that. This discrepancy is due to different behavior in different regions of the stress-strain curve. The deformation of polyurethane foam has three regions which can be distinguished during uniaxial compression:
    a) Initial elastic deformation: In the first stage, the polyurethane foam deforms in a linear elastic manner due to cell wall bending, which accounts for less than 5% of the entire deformation as shown in graph below:

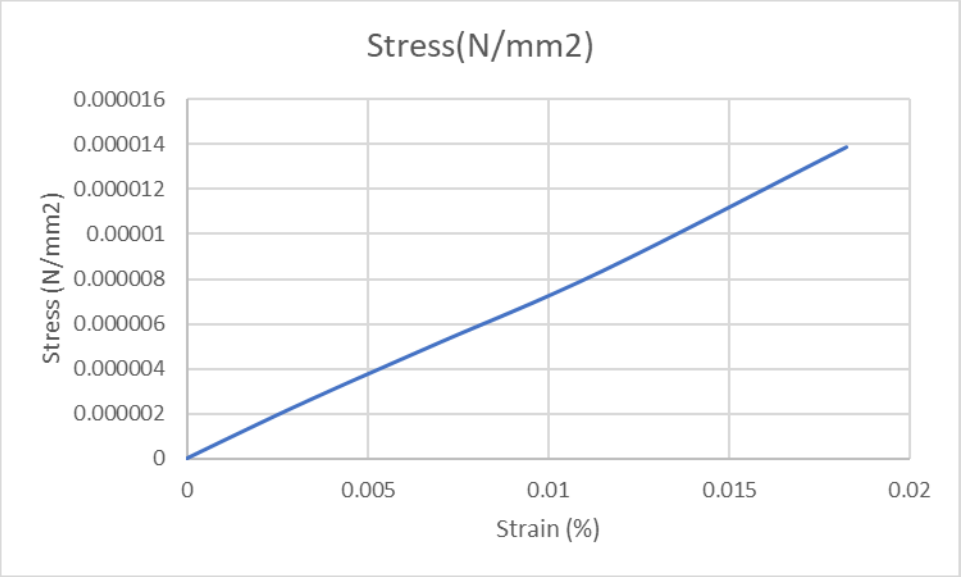

Figure 27 Stress-Strain Graph Showing Region 1

a) Collapse deformation: In the course of the second stage, there is a plateau of deformation at almost constant stress. The cell walls, which are like thin tubes or plates, lose their stability and cause large deformations. During this stress plateau phase, the polyurethane foam undergoes large compressive strains and absorbs a considerable amount of specific energy. The corresponding stress for strain increase from 10% to ~55% in Figure 25 shows this region

b) Compaction deformation: In the third stage, a region of densification occurs where the cell walls crush together, resulting in a rapid increase in compressive stress. The final part of stress-strain curve from about ~55% to 80% strain shows this region.

Effect of Height of Cone on Reaction Force

To perform a parametric comparison of geometric property of cone, same static compressive analysis was also performed for a cone of different height and the result of reaction force for same displacement was compared as shown in the graph below

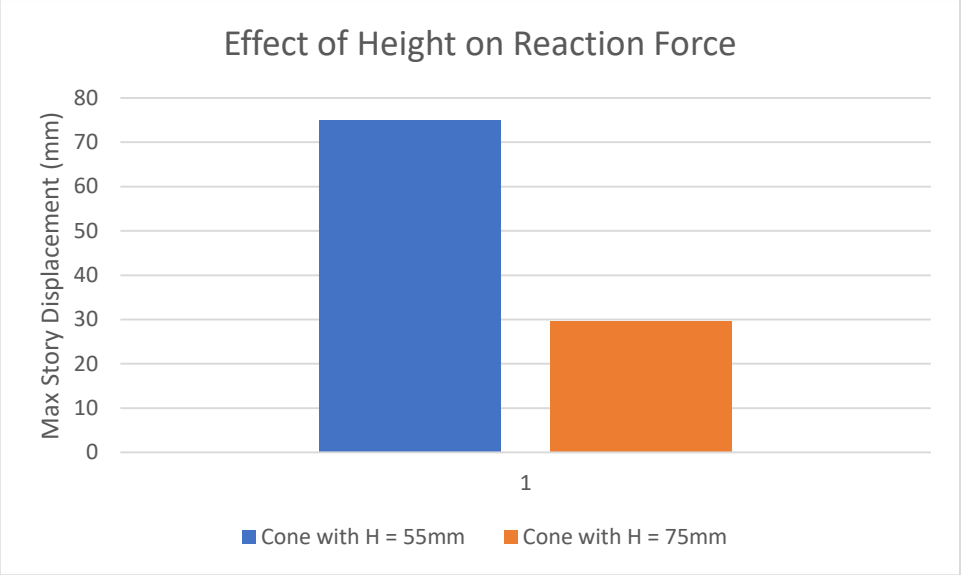

Figure 28 Cone Height Comparison Chart

It can be clearly seen that a cone with less height and same base exhibits more force for the same compressive strain. This results is also in line with a study conducted by (Luo, Wierschem, Fahnestock, Bergman, et al., 2014)

Effect of Model Strain Energy Potential Order

Ogden model for hyperelastic materials can be applied in increasing orders of strain energy potential to capture the behavior of the material more accurately. The obvious tradeoff is accuracy vs computational cost. The following force-displacement graph shows a comparison of Ogden models for strain energy potential of N=2 and N=3.

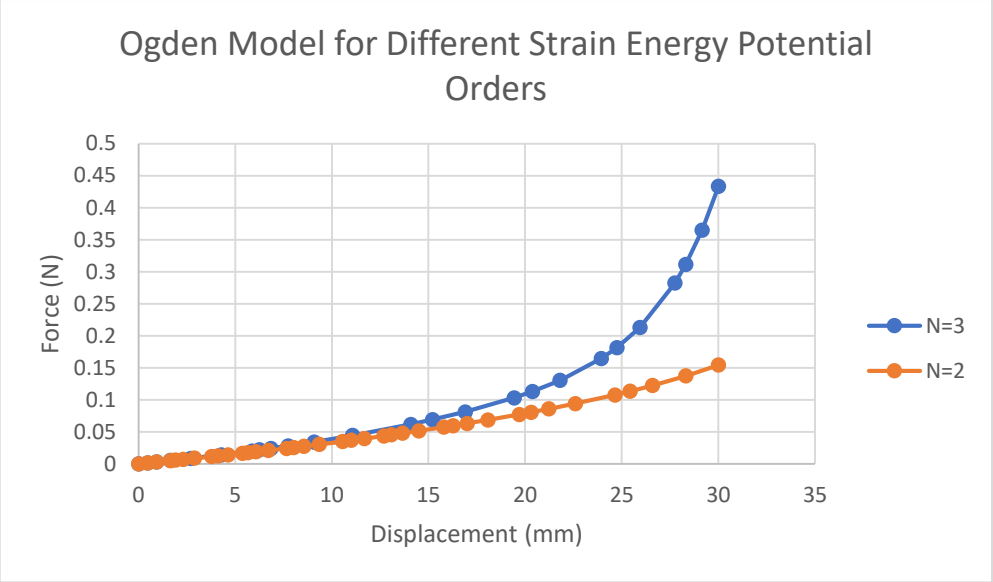

Figure 29 Ogden Strain Energy Potential Order

It is clear from the above graph that for potential order of N=3, the model can capture the flexural behavior of the material much better than the potential order of N=2

Mesh Independence

To perform mesh independence study, the force was calculated for 40% strain while gradually decreasing the mesh element size. The below graph is a comparison of results for force at 40% strain for different element sizes

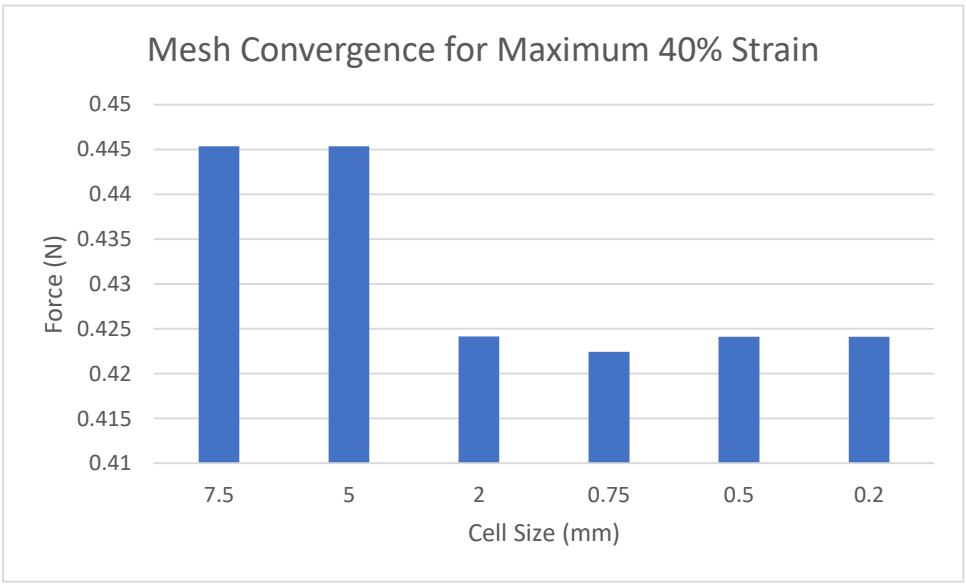

The graph exhibits that for element size of less than 0.5mm, the results start showing a consistent behavior and anything below 0.2mm element size is just adding to the computational cost.

Study Validation

The widely acknowledged validation method for a hyperelastic polymer finite element analysis is to compare it with experimental results. Since our study is entirely based on using computational resources only, the validation method most suitable was to compare the results with an already established study. The material described in previous chapter was used in a study by (Ju et al., 2015) to determine model coefficients for material under study. They first do an experimental study and then validate the results of their analysis.

In our study, we compare out force-strain graph with that of the experimentally drawn graph in the study and try to draw conclusions. The graph is shown below followed by conclusions.

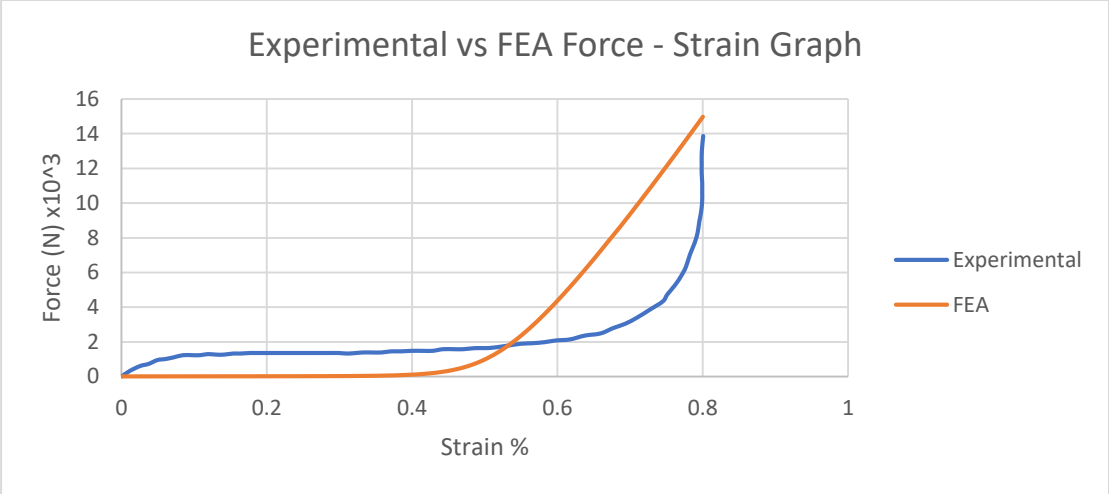

Figure 30 Experimental vs FEA Force-Strain Graph

The conclusions drawn from the above graph are:

1. The FEA simulation was successful in capturing the behavior of material up to the exhibition of single flexural point.
2. It clearly demonstrated at least the 2nd and 3rd regions in hyperelastic material deformation but couldn't clearly capture the 1st region as well.
3. The deviation from experimental results may be attributed to the following limitations:
    a. The experimental data wasn't available readily in tabular form but was extracted from the plotted graph in the study and may be prone to erroneous readings.
    b. The information about other simulation parameters, such as; mesh data, boundary conditions and contact parameters, used in the referenced study was not available which may have affected the results.
    c. The simulation only accounts for the hyperelastic behavior of the material and ignores the viscoelastic behavior which is an oversimplification of the material behavior and requires a more robust analysis to cater to it.

Effectiveness of NES device with Elastomeric Springs in Multi Degree-of-Freedom Systems

In this part, we will compare the story response for the first 2 modes of a 10-story frame structure in ETABS with and without Elastomeric NES. The data for the frame structure is tabulated as follows:

Table 6 Story Data

Story Data		
Name	**Height**	**Elevation**
	mm	mm
Story9	5000	45000
Story8	5000	40000
Story7	5000	35000
Story6	5000	30000
Story5	5000	25000
Story4	5000	20000
Story3	5000	15000
Story2	5000	10000
Story1	5000	5000
Base	0	0

Table 7 Material Properties

Material Properties - Summary					
Name	**Type**	**E**	**ν**	**Unit Weight**	**Design Strengths**
		MPa		kN/m³	
4000Psi	Concrete	24855.58	0.2	23.5631	Fc=27.58 MPa
A416Gr270	Tendon	196500.6	0	76.9729	Fy=1689.91 MPa, Fu=1861.58 MPa
A615Gr60	Rebar	199947.98	0.3	76.9729	Fy=413.69 MPa, Fu=620.53 MPa
A992Fy50	Steel	199947.98	0.3	76.9729	Fy=344.74 MPa, Fu=448.16 MPa

Table 8 Story Mass

Mass Summary by Story	
Story	**Mass**
	kg
Story9	29397.55
Story8	33003.2

Story7	33003.2
Story6	33003.2
Story5	33003.2
Story4	33003.2
Story3	33003.2
Story2	33003.2
Story1	33003.2
Base	5565.87

Table 9 Modal Properties and Frequencies

Modal Periods and Frequencies			
Case	**Mode**	**Period**	**Frequency**
		sec	cyc/sec
Modal	1	1.773	0.564
Modal	2	1.414	0.707
Modal	3	1.235	0.81

Modal	4	0.565	1.769
Modal	5	0.443	2.255
Modal	6	0.397	2.522
Modal	7	0.312	3.205
Modal	8	0.24	4.172
Modal	9	0.223	4.484
Modal	10	0.21	4.767

The device is employed in the structure by imparting its load-displacement curve to a link type element in ETABS and installing the link in the frame structure. Below graphs represent the story response plots:

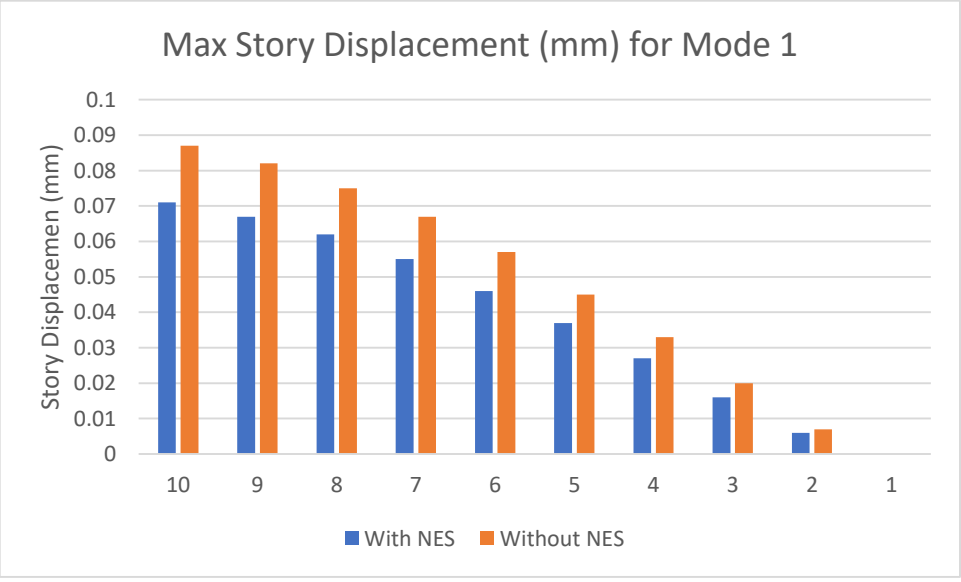

Figure 31 Max Story Displacement for Mode1

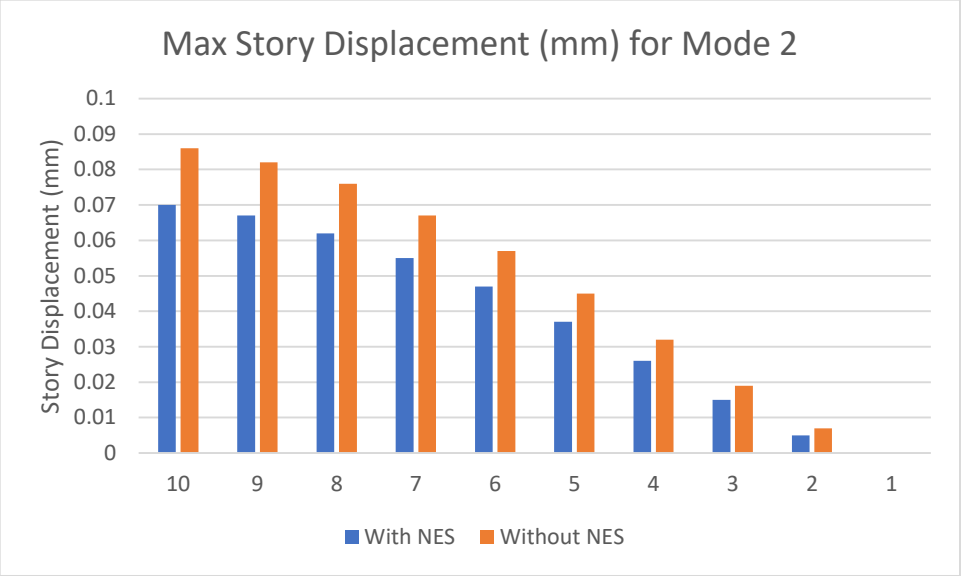

Figure 32 Max Story Displacement for Mode2

From the above graphs, it can be clearly demonstrated that the maximum story displacement for structure with NES is less than that of structure without NES which shows that device has the capability to mitigate maximum story displacement of a frame structure across multiple modes.

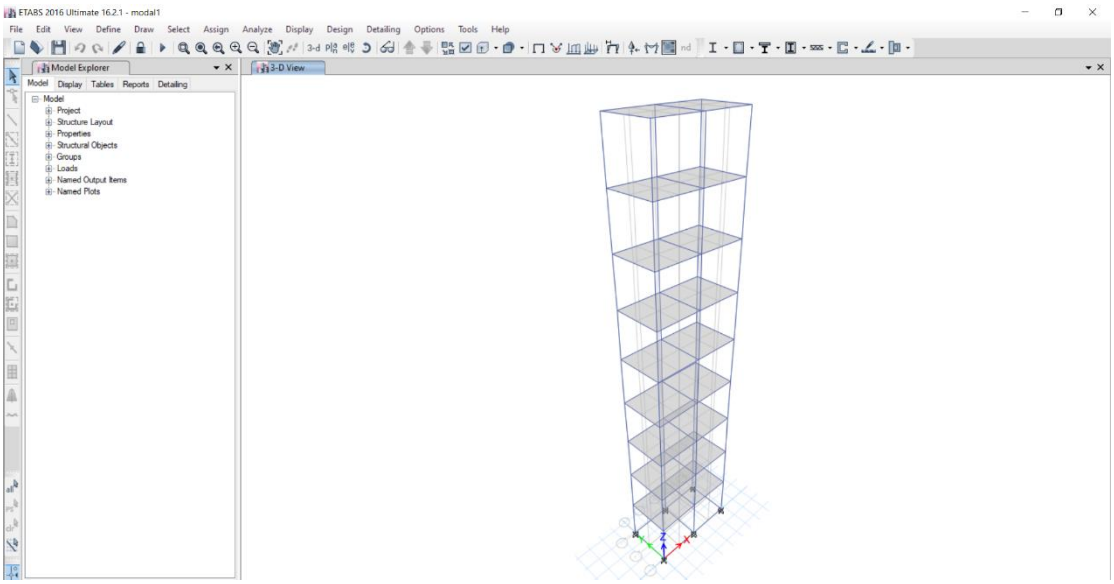

Figure 33 Frame Structure without NESs'

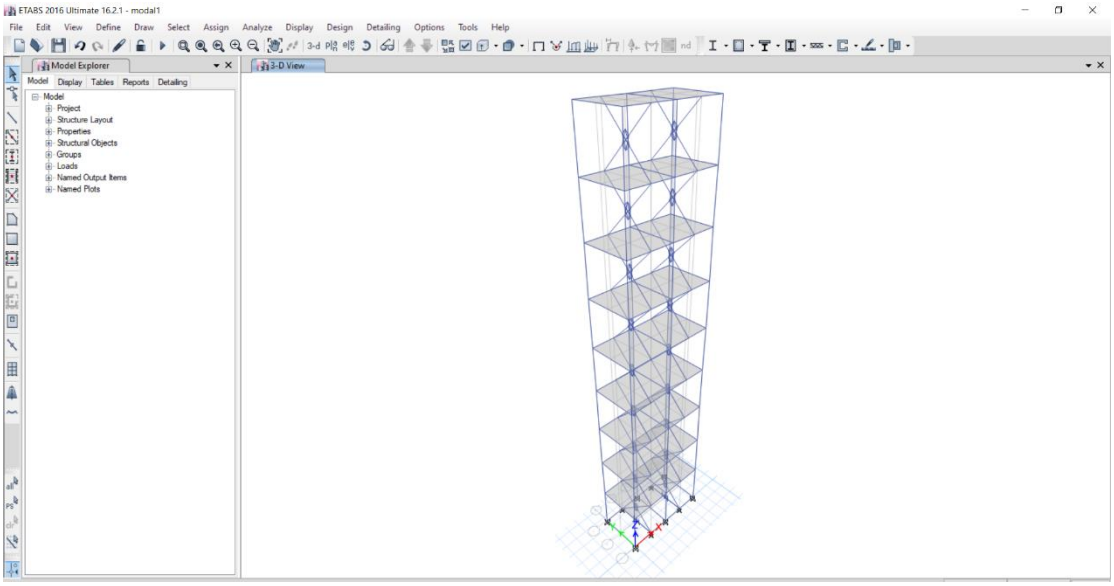

Figure 34 Frame Structure With NESs'

Chapter 5: Conclusions and Future Recommendations

Conclusion

The results of the study were able to demonstrate the potential of hyperelastic polyurethane materials as nonlinear elastomeric springs for nonlinear energy sinks as a vibration mitigation device in civil structures. The results show that these types of material are capable of exhibiting a highly nonlinear stiffness behavior under compression and therefore, can be further investigated as essentially nonlinear springs in such devices.

The study also demonstrated that the Ogden hyperelastic model is capable of simulating the behavior of hyperelastic materials under very large strains.

Finally, it shows that the validation of simulation results is dependent upon experimental results and therefore, experimental data is crucial for such studies, especially the ones involving geometric nonlinearities as well as material nonlinearity.

Future Recommendations

The following recommendations for future work can be drawn from this study:

- Parametric experimental studies of different hyperelastic materials having nonlinear geometric properties to build a database.
- Use of Time History Analysis for structures using NES devices for more accurate and precise evaluation of their effectiveness.
- Conducting a fatigue analysis for hyperelastic materials under compression
- Use of Machine Learning methods to determine device parameters.

References

Abdel-Rohman, M. (1984). Optimal design of active TMD for buildings control. *Building and Environment*, *19*(3), 191–195. https://doi.org/10.1016/0360-1323(84)90026-X

Agathoklis Giaralis, & Alexandros Taflanidis. (n.d.). Robust reliability-based design of seismically excited tuned mass-damper-inerter (TMDI) equipped MDOF structures with uncertain properties. *Conference: 6th European Conference on Structural Control*.

Al-Shudeifat, M. A. (2014). Highly efficient nonlinear energy sink. *Nonlinear Dynamics*, *76*(4), 1905–1920. https://doi.org/10.1007/s11071-014-1256-x

Andersen, D., Starosvetsky, Y., Vakakis, A., & Bergman, L. (2012). Dynamic instabilities in coupled oscillators induced by geometrically nonlinear damping. *Nonlinear Dynamics*, *67*(1), 807–827. https://doi.org/10.1007/s11071-011-0028-0

Benarous, N., & Gendelman, O. V. (2016). Nonlinear energy sink with combined nonlinearities: Enhanced mitigation of vibrations and amplitude locking phenomenon. *Proceedings of the Institution of Mechanical Engineers, Part C: Journal of Mechanical Engineering Science*, *230*(1), 21–33. https://doi.org/10.1177/0954406215579930

Chang, J. C. H., & Soong, T. T. (1980). Structural Control Using Active Tuned Mass Dampers. *Journal of the Engineering Mechanics Division*, *106*(6), 1091–1098. https://doi.org/10.1061/JMCEA3.0002652

Ding, H., & Chen, L.-Q. (2020). Designs, analysis, and applications of nonlinear energy sinks. *Nonlinear Dynamics*, *100*(4), 3061–3107. https://doi.org/10.1007/s11071-020-05724-1

El Ouni, M. H., Abdeddaim, M., Elias, S., & Kahla, N. Ben. (2022). Review of Vibration Control Strategies of High-Rise Buildings. In *Sensors* (Vol. 22, Issue 21). MDPI. https://doi.org/10.3390/s22218581

Elias, S., Djerouni, S., De Domenico, D., Abdeddaim, M., & El Ouni, M. H. (2023). Seismic response control of building structures under pulse-type ground motions by active vibration controller. *Journal of Low Frequency Noise, Vibration and Active Control*, *42*(1), 345–367. https://doi.org/10.1177/14613484221130192

Elias, S., & Matsagar, V. (2017). Research developments in vibration control of structures using passive tuned mass dampers. In *Annual Reviews in Control* (Vol. 44, pp. 129–156). Elsevier Ltd. https://doi.org/10.1016/j.arcontrol.2017.09.015

El-Khoury, O., & Adeli, H. (2013). Recent Advances on Vibration Control of Structures Under Dynamic Loading. In *Archives of Computational Methods in Engineering* (Vol. 20, Issue 4, pp. 353–360). https://doi.org/10.1007/s11831-013-9088-2

Gajewski, M., Szczerba, R., & Jemioło, S. (2015). Modelling of elastomeric bearings with application of Yeoh hyperelastic material model. *Procedia Engineering*, *111*, 220–227. https://doi.org/10.1016/j.proeng.2015.07.080

GEORGIADIS, F., VAKAKIS, A. F., MCFARLAND, D. M., & BERGMAN, L. (2005). SHOCK ISOLATION THROUGH PASSIVE ENERGY PUMPING CAUSED BY NONSMOOTH NONLINEARITIES.

International Journal of Bifurcation and Chaos, *15*(06), 1989–2001. https://doi.org/10.1142/S0218127405013101

Gourdon, E., Alexander, N. A., Taylor, C. A., Lamarque, C. H., & Pernot, S. (2007). Nonlinear energy pumping under transient forcing with strongly nonlinear coupling: Theoretical and experimental results. *Journal of Sound and Vibration*, *300*(3–5), 522–551. https://doi.org/10.1016/j.jsv.2006.06.074

Guclu, R., & Yazici, H. (2008). Vibration control of a structure with ATMD against earthquake using fuzzy logic controllers. *Journal of Sound and Vibration*, *318*(1–2), 36–49. https://doi.org/10.1016/j.jsv.2008.03.058

Huri, D., & Mankovits, T. (2018). Comparison of the material models in rubber finite element analysis. *IOP Conference Series: Materials Science and Engineering*, *393*, 012018. https://doi.org/10.1088/1757-899X/393/1/012018

Ismail, R., Ibrahim, A., & Hamid, H. Ab. (2014). A Review of Magnetorheological Elastomers: Characterization Properties for Seismic Protection. In *InCIEC 2013* (pp. 237–248). Springer Singapore. https://doi.org/10.1007/978-981-4585-02-6_21

Ju, M. L., Jmal, H., Dupuis, R., & Aubry, E. (2015). Visco-hyperelastic constitutive model for modeling the quasi-static behavior of polyurethane foam in large deformation. *Polymer Engineering and Science*, *55*(8), 1795–1804. https://doi.org/10.1002/pen.24018

Kadlowec, J., Wineman, A., & Hulbert, G. (2003). Elastomer bushing response: Experiments and finite element modeling. *Acta Mechanica*, *163*(1–2), 25–38. https://doi.org/10.1007/s00707-003-1018-1

Kang, S. S., Choi, K., Nam, J. Do, & Choi, H. J. (2020). Magnetorheological elastomers: Fabrication, characteristics, and applications. In *Materials* (Vol. 13, Issue 20, pp. 1–24). MDPI AG. https://doi.org/10.3390/ma13204597

Kareem, A., Kijewski, T., & Tamura, Y. (1999). Mitigation of motions of tall buildings with specific examples of recent applications. *Wind and Structures*, *2*(3), 201–251. https://doi.org/10.12989/was.1999.2.3.201

Kobori, T., Koshika, N., Yamada, K., & Ikeda, Y. (1991). Seismic-response-controlled structure with active mass driver system. Part 1: Design. *Earthquake Engineering & Structural Dynamics*, *20*(2), 133–149. https://doi.org/10.1002/eqe.4290200204

Lee, J. H., Singer, J. P., & Thomas, E. L. (2012). Micro-/nanostructured mechanical metamaterials. In *Advanced Materials* (Vol. 24, Issue 36, pp. 4782–4810). https://doi.org/10.1002/adma.201201644

Liu, I.-S. (2012). A note on the Mooney–Rivlin material model. *Continuum Mechanics and Thermodynamics*, *24*(4–6), 583–590. https://doi.org/10.1007/s00161-011-0197-6

Luo, J., Wierschem, N. E., Fahnestock, L. A., Bergman, L. A., Spencer, B. F., AL-Shudeifat, M., McFarland, D. M., Quinn, D. D., & Vakakis, A. F. (2014). Realization of a Strongly Nonlinear Vibration-Mitigation Device Using Elastomeric Bumpers. *Journal of Engineering Mechanics*, *140*(5). https://doi.org/10.1061/(asce)em.1943-7889.0000692

Luo, J., Wierschem, N. E., Fahnestock, L. A., Spencer, B. F., Quinn, D. D., Mcfarland, D. M., Vakakis, A. F., & Bergman, L. A. (2014). Design, simulation, and large-scale testing of an innovative vibration mitigation device employing essentially nonlinear elastomeric springs. *Earthquake*

Engineering and Structural Dynamics, *43*(12), 1829–1851. https://doi.org/10.1002/eqe.2424

Luo, J., Wierschem, N. E., Hubbard, S. A., Fahnestock, L. A., Dane Quinn, D., Michael McFarland, D., Spencer, B. F., Vakakis, A. F., & Bergman, L. A. (2014). Large-scale experimental evaluation and numerical simulation of a system of nonlinear energy sinks for seismic mitigation. *Engineering Structures*, *77*, 34–48. https://doi.org/10.1016/J.ENGSTRUCT.2014.07.020

McFarland, D. M., Kerschen, G., Kowtko, J. J., Lee, Y. S., Bergman, L. A., & Vakakis, A. F. (2005). Experimental investigation of targeted energy transfers in strongly and nonlinearly coupled oscillators. *The Journal of the Acoustical Society of America*, *118*(2), 791–799. https://doi.org/10.1121/1.1944649

Nicholas E. Wierschem. (2014). *Targeted energy transfer using nonlinear energy sinks for the attenuation of transient loads on building structures*.

Nonlinear Targeted Energy Transfer in Mechanical and Structural Systems (Vol. 156). (2009). Springer Netherlands. https://doi.org/10.1007/978-1-4020-9130-8

Pawlikowski, M. (2014). Non-linear approach in visco-hyperelastic constitutive modelling of polyurethane nanocomposite. *Mechanics of Time-Dependent Materials*, *18*(1), 1–20. https://doi.org/10.1007/s11043-013-9208-2

Qi, H. J., & Boyce, M. C. (n.d.). *Stress-Strain Behavior of Thermoplastic Polyurethane*.

Raze, G., & Kerschen, G. (2020). Multimodal vibration damping of nonlinear structures using multiple nonlinear absorbers. *International Journal of Non-Linear Mechanics*, *119*, 103308. https://doi.org/10.1016/j.ijnonlinmec.2019.103308

Samali, B., Yang, J. N., & Yeh, C. T. (1985). Control of Lateral-Torsional Motion of Wind-Excited Buildings. *Journal of Engineering Mechanics*, *111*(6), 777–796. https://doi.org/10.1061/(ASCE)0733-9399(1985)111:6(777)

Sheikhi, M. R., Shamsadinlo, B., Ünver, Ö., & Gürgen, S. (2021). Finite element analysis of different material models for polyurethane elastomer using estimation data sets. *Journal of the Brazilian Society of Mechanical Sciences and Engineering*, *43*(12). https://doi.org/10.1007/s40430-021-03279-9

Standard Test Methods for Rubber Properties in Compression 1 2. Referenced Documents 2.1 ASTM Standards: D 3183 Practice for Rubber-Preparation of Pieces for Test Purposes from Products 2 D 3767 Practice for Rubber-Measurement of Dimen-sions 2 D 4483 Practice for Determining Precision for Test Method Standards in the Rubber and Carbon Black Industries 2 E 4 Practices for Force Verification of Testing Machines 3. (n.d.).

Stress Concentration. (n.d.).

Ümütlü, R. C., Ozturk, H., & Bidikli, B. (2021). A robust adaptive control design for active tuned mass damper systems of multistory buildings. *Journal of Vibration and Control*, *27*(23–24), 2765–2777. https://doi.org/10.1177/1077546320966236

Wang, A.-P., & Lin, Y.-H. (2007). Vibration control of a tall building subjected to earthquake excitation. *Journal of Sound and Vibration*, *299*(4–5), 757–773. https://doi.org/10.1016/j.jsv.2006.07.016

Wu, J. C., & Yang, J. N. (1998). Active Control of Transmission Tower under Stochastic Wind. *Journal of Structural Engineering*, *124*(11), 1302–1312. https://doi.org/10.1061/(ASCE)0733-9445(1998)124:11(1302)

Yamamoto, M., Aizawa, S., Higashino, M., & Toyama, K. (2001). Practical applications of active mass dampers with hydraulic actuator. *Earthquake Engineering & Structural Dynamics*, *30*(11), 1697–1717. https://doi.org/10.1002/eqe.88

Yanik, A. (2019). Absolute Instantaneous Optimal Control Performance Index for Active Vibration Control of Structures under Seismic Excitation. *Shock and Vibration*, *2019*, 1–13. https://doi.org/10.1155/2019/4207427

Yanik, A., Aldemir, U., & Bakioglu, M. (2014). A new active control performance index for vibration control of three-dimensional structures. *Engineering Structures*, *62–63*, 53–64. https://doi.org/10.1016/j.engstruct.2014.01.009